

Widely-Linear MMSE Estimation of Complex-Valued Graph Signals

Alon Amar and Tirza Routtenberg, *Senior Member, IEEE*

Abstract—In this paper, we consider the problem of recovering random graph signals with complex values. For general Bayesian estimation of complex-valued vectors, it is known that the widely-linear minimum mean-squared-error (WLMMSE) estimator can achieve a lower mean-squared-error (MSE) than that of the linear minimum MSE (LMMSE) estimator. Inspired by the WLMMSE estimator, in this paper we develop the graph signal processing (GSP)-WLMMSE estimator, which minimizes the MSE among estimators that are represented as a two-channel output of a graph filter, i.e. widely-linear GSP estimators. We discuss the properties of the proposed GSP-WLMMSE estimator. In particular, we show that the MSE of the GSP-WLMMSE estimator is always equal to or lower than the MSE of the GSP-LMMSE estimator. The GSP-WLMMSE estimator is based on *diagonal* covariance matrices in the graph frequency domain, and thus has reduced complexity compared with the WLMMSE estimator. This property is especially important when using the sample-mean versions of these estimators that are based on a training dataset. We then state conditions under which the low-complexity GSP-WLMMSE estimator coincides with the WLMMSE estimator. In the simulations, we investigate two synthetic estimation problems (with linear and nonlinear models) and the problem of state estimation in power systems. For these problems, it is shown that the GSP-WLMMSE estimator outperforms the GSP-LMMSE estimator and achieves similar performance to that of the WLMMSE estimator.

Index Terms—Widely-linear minimum mean-squared-error (WLMMSE) estimator, graph signal processing (GSP), graph filters, improper complex-valued random signals

I. INTRODUCTION

Graph signal processing (GSP) theory extends concepts and techniques from traditional digital signal processing (DSP) to data indexed by generic graphs, including the graph Fourier transform (GFT), graph filter design [1], [2], and sampling of graph signals [3], [4]. In this context, the development of GSP methods for the recovery (or estimation) of graph signals is a fundamental task with both practical and theoretical importance [5], [6]. However, most works have focused on real-valued graph signals. Complex-valued graph signals arise in several real-world applications, such as multi-agent systems [7], wireless communication systems [8], voltage and power phasors in electrical networks [9]–[11], and probabilistic graphical models with complex-valued multivariate Gaussian vectors [12]. Despite the widespread use of complex-valued graph signals, their recovery is a crucial problem that has not been well explored.

A. Amar is an adjunct instructor at the Faculty of Electrical & Computer Engineering, Technion, Haifa, Israel. T. Routtenberg is with the School of Electrical and Computer Engineering, Ben-Gurion University of the Negev, Beer Sheva, Israel. e-mail: amar@technion.ac.il, tirzar@bgu.ac.il. This work has been submitted to the IEEE for possible publication. Copyright may be transferred without notice, after which this version may no longer be accessible.

This work is partially supported by the Israeli Ministry of National Infrastructure, Energy, and Water Resources.

In processing general complex-valued random vectors, standard statistical signal processing approaches typically impose a restrictive assumption on these vectors in the form of properness or second-order circularity [13]. However, this assumption does not necessarily hold, and in various applications the data is noncircular or improper (i.e. the signals have linear correlations with their own complex conjugates [14]). This situation arises, for example, through power imbalance and correlation in data channels [15], [16]. Various tools for the processing of noncircular complex-valued signals for different tasks were proposed in the literature [17]–[20], based on augmented complex statistics [14], [21]. In the context of parameter estimation, it has been shown that if the observation and/or the parameter of interest are improper, widely-linear estimators can outperform conventional linear estimators. In particular, the widely-linear minimum mean-squared-error (WLMMSE) estimator, first proposed in [19], outperforms the linear minimum mean-squared-error (LMMSE) estimator for improper random vectors. However, widely-linear estimation of graph signals by GSP tools has not been analyzed.

Graph filters have been used for many signal processing tasks, such as classification [22], denoising [23], and anomaly detection [10]. Model-based recovery of a graph signal from noisy measurements by graph filters for *linear* models, usually with *real-valued* data, was treated in [23]–[26]. The graphical Wiener filter was developed in [26] and in [27] for real and for proper complex signals, respectively. Nonlinear methods, such as the nonlinear graph filters that were considered in [28], require higher-order statistics that are not completely specified in the general case, and have significantly greater computational complexity. Graph neural network approaches [29], [30] require extensive training sets and result in nonlinear estimators with high computational complexity. Fitting graph-based models to given data was considered in [31]–[33]. Based on the fitted graph-based model, one can implement different simple recovery algorithms. However, model-fitting approaches aim to minimize the modeling error and, in general, have significantly lower performance than estimators that minimize the estimation error directly.

In our previous work in [6] we proposed the GSP-linear minimum mean-squared-error (GSP-LMMSE) estimator for the recovery of real-valued graph signals. The GSP-LMMSE estimator minimizes the mean-squared-error (MSE) among the subset of estimators that are represented as an output of a graph filter. It was shown in [6] that the GSP-LMMSE estimator has a lower computational complexity than the LMMSE estimator, and requires less training data when there is a need to estimate the covariance matrices. It also has graph filter implementations that are adaptive to changes in the graph topology, outperforming the LMMSE estimator under such changes. Our goal in this paper is to obtain a low-complexity

estimator for the general nonlinear case that has optimal MSE performance for the recovery of *complex-valued* graph signals. In this paper, we describe a Bayesian framework for the widely-linear estimation of complex-valued graph signals by using GSP filters. Thus, the proposed framework takes advantage of the power of both complex-domain nonlinear processing and GSP theory. In particular, we develop the GSP-WLMMSE estimator, which is the estimator that achieves the minimum MSE within the class of widely-linear estimators that are the output of graph filters. We show that using widely-linear graph filtering instead of strictly linear graph filtering can yield significant MSE improvements in the estimation of graph signals with complex data. We discuss more aspects of the proposed GSP-WLMMSE estimator, including the orthogonality principle, computational complexity, relation with existing estimators, and its behavior for the special cases of proper signals and data, maximal improper observation vectors, and real-valued unknown graph signals (Subsection IV-C). In the simulations, it is shown that the GSP-WLMMSE estimator has a significantly lower MSE than that of the LMMSE estimator for synthetic examples and for the problem of state estimation in power systems.

Organization: The rest of this paper is organized as follows. In Section II we introduce the basics of GSP and widely-linear estimation required for this paper. In Section III, we formulate the estimation problem and develop the proposed GSP-WLMMSE estimator for improper graph signals and discuss its properties. Some special cases are presented in Section IV. Simulations are shown in Section V. Finally, the paper is concluded in Section VI.

Notation: We use boldface lowercase letters to denote vectors and boldface capital letters for matrices. The identity matrix is denoted by \mathbf{I} and $\|\cdot\|$ denotes the Euclidean l_2 -norm of vectors. The symbols $(\cdot)^*$, $(\cdot)^T$, and $(\cdot)^H$ represent the conjugate, transpose, and conjugate transpose operators, respectively. The symbol $(\cdot)^{-*}$ denotes the conjugate of the inverse matrix. We use $\text{tr}(\mathbf{A})$ to denote the trace of the matrix \mathbf{A} . For a vector \mathbf{a} , $\text{diag}(\mathbf{a})$ is a diagonal matrix whose i th diagonal entry is a_i ; when applied to a matrix, $\text{diag}(\mathbf{A})$ is a vector collecting the diagonal elements of \mathbf{A} . In addition, $\text{ddiag}(\mathbf{A}) = \text{diag}(\text{diag}(\mathbf{A}))$. Two zero-mean random vectors $\mathbf{a} \in \mathbb{C}^N$ and $\mathbf{b} \in \mathbb{C}^N$ are defined as orthogonal if $\mathbb{E}[\mathbf{a}^H \mathbf{b}] = 0$, which is denoted as $\mathbf{a} \perp \mathbf{b}$. For two zero-mean complex-valued vectors \mathbf{a} and \mathbf{b} , we denote the cross-covariance and the complementary cross-covariance matrices between them as

$$\mathbf{\Gamma}_{\mathbf{ab}} = \mathbb{E}[\mathbf{ab}^H] \quad (1a)$$

and

$$\mathbf{C}_{\mathbf{ab}} = \mathbb{E}[\mathbf{ab}^T], \quad (1b)$$

respectively. The complementary cross-covariance matrix, $\mathbf{C}_{\mathbf{ab}}$, is also known as the pseudo or conjugate covariance.

II. BACKGROUND

In this section, we briefly present background on WLMMSE estimation (Subsection II-A), the GSP notations (Subsection II-B), and the GSP-LMMSE estimator (Subsection II-C).

A. WLMMSE Estimation

Consider the problem of estimating an N -dimensional zero-mean signal $\mathbf{x} \in \mathbb{C}^N$ from an N -dimensional zero-mean measurement $\mathbf{y} \in \mathbb{C}^N$. In order for an estimator to utilize all the available second-order information in both proper and improper signals, the estimators should depend on both the signals and their complex conjugates, i.e. on the augmented vector $\underline{\mathbf{y}} = [\mathbf{y}^T \ \mathbf{y}^H]^T$. It can be seen that the augmented auto-covariance matrix satisfies

$$\mathbf{\Gamma}_{\underline{\mathbf{y}}\underline{\mathbf{y}}} = \mathbb{E}[\underline{\mathbf{y}}\underline{\mathbf{y}}^H] = \begin{bmatrix} \mathbf{\Gamma}_{\mathbf{y}\mathbf{y}} & \mathbf{C}_{\mathbf{y}\mathbf{y}} \\ \mathbf{C}_{\mathbf{y}\mathbf{y}}^* & \mathbf{\Gamma}_{\mathbf{y}\mathbf{y}}^* \end{bmatrix} = \mathbf{\Gamma}_{\underline{\mathbf{y}}\underline{\mathbf{y}}}^H, \quad (2)$$

where the cross-covariance and the complementary cross-covariance matrices are $\mathbf{\Gamma}_{\mathbf{y}\mathbf{y}} = \mathbb{E}[\mathbf{y}\mathbf{y}^H]$ and $\mathbf{C}_{\mathbf{y}\mathbf{y}} = \mathbb{E}[\mathbf{y}\mathbf{y}^T]$, as defined in (1). If the complementary covariance matrix vanishes, i.e. $\mathbf{C}_{\mathbf{y}\mathbf{y}} = \mathbf{0}$, the vector \mathbf{y} is called a proper vector, while when $\mathbf{C}_{\mathbf{y}\mathbf{y}} \neq \mathbf{0}$ it is called an improper vector. We assume in this paper that $\mathbf{\Gamma}_{\mathbf{y}\mathbf{y}}$ is a non-singular matrix.

For improper random variables, the widely-linear estimators can be used to achieve better performance than that of the LMMSE estimator. In particular, a widely-linear estimator of the signal \mathbf{x} based on the measurement vector \mathbf{y} has the form

$$\hat{\mathbf{x}} = \mathbf{H}_1 \mathbf{y} + \mathbf{H}_2 \mathbf{y}^*. \quad (3)$$

In order to find the WLMMSE estimator, the filters $\mathbf{H}_1, \mathbf{H}_2 \in \mathbb{C}^{N \times N}$ are determined by minimizing the MSE as follows:

$$\begin{aligned} \min_{\mathbf{H}_1, \mathbf{H}_2 \in \mathbb{C}^{N \times N}} \mathbb{E}[\|\hat{\mathbf{x}} - \mathbf{x}\|^2] \\ = \min_{\mathbf{H}_1, \mathbf{H}_2 \in \mathbb{C}^{N \times N}} \mathbb{E}[\|\mathbf{H}_1 \mathbf{y} + \mathbf{H}_2 \mathbf{y}^* - \mathbf{x}\|^2]. \end{aligned} \quad (4)$$

The solution of (4) is given by [19]

$$\hat{\mathbf{H}}_1 = (\mathbf{\Gamma}_{\mathbf{x}\mathbf{y}} - \mathbf{C}_{\mathbf{x}\mathbf{y}}(\mathbf{\Gamma}_{\mathbf{y}\mathbf{y}}^{-1})^*(\mathbf{C}_{\mathbf{y}\mathbf{y}})^*)\mathbf{P}_{\mathbf{y}\mathbf{y}}^{-1} \quad (5)$$

$$\hat{\mathbf{H}}_2 = (\mathbf{C}_{\mathbf{x}\mathbf{y}} - \mathbf{\Gamma}_{\mathbf{x}\mathbf{y}}\mathbf{\Gamma}_{\mathbf{y}\mathbf{y}}^{-1}\mathbf{C}_{\mathbf{y}\mathbf{y}})(\mathbf{P}_{\mathbf{y}\mathbf{y}}^{-1})^*, \quad (6)$$

where the Schur complement of the matrix $\mathbf{\Gamma}_{\underline{\mathbf{y}}\underline{\mathbf{y}}}$, which is the error covariance matrix for linearly estimating \mathbf{y} from \mathbf{y}^* , is

$$\mathbf{P}_{\mathbf{y}\mathbf{y}} \triangleq \mathbf{\Gamma}_{\mathbf{y}\mathbf{y}} - \mathbf{C}_{\mathbf{y}\mathbf{y}}(\mathbf{\Gamma}_{\mathbf{y}\mathbf{y}}^{-1})^*(\mathbf{C}_{\mathbf{y}\mathbf{y}})^*. \quad (7)$$

By substituting (5) and (6) in (3), we obtain that the WLMMSE estimator is

$$\begin{aligned} \hat{\mathbf{x}}^{\text{WLMMSE}} &= (\mathbf{\Gamma}_{\mathbf{x}\mathbf{y}} - \mathbf{C}_{\mathbf{x}\mathbf{y}}(\mathbf{\Gamma}_{\mathbf{y}\mathbf{y}}^{-1})^*\mathbf{C}_{\mathbf{y}\mathbf{y}}^*)\mathbf{P}_{\mathbf{y}\mathbf{y}}^{-1}\mathbf{y} \\ &\quad + (\mathbf{C}_{\mathbf{x}\mathbf{y}} - \mathbf{\Gamma}_{\mathbf{x}\mathbf{y}}\mathbf{\Gamma}_{\mathbf{y}\mathbf{y}}^{-1}\mathbf{C}_{\mathbf{y}\mathbf{y}})(\mathbf{P}_{\mathbf{y}\mathbf{y}}^{-1})^*\mathbf{y}^*. \end{aligned} \quad (8)$$

By using the fact that $\mathbb{E}[\mathbf{y}\mathbf{y}^H] = \mathbf{\Gamma}_{\mathbf{y}\mathbf{y}}$ and $\mathbb{E}[\mathbf{y}\mathbf{y}^T] = \mathbf{C}_{\mathbf{y}\mathbf{y}}$, it can be verified that the corresponding MSE of the WLMMSE estimator is [19]

$$\begin{aligned} \varepsilon_{WL}^2 &\triangleq \mathbb{E}[\|\hat{\mathbf{x}}^{\text{WLMMSE}} - \mathbf{x}\|^2] \\ &= \text{tr}\left(\mathbf{\Gamma}_{\mathbf{x}\mathbf{x}} - \begin{bmatrix} \hat{\mathbf{H}}_1 & \hat{\mathbf{H}}_2 \end{bmatrix} \mathbf{\Gamma}_{\underline{\mathbf{y}}\underline{\mathbf{y}}} \begin{bmatrix} \hat{\mathbf{H}}_1^H \\ \hat{\mathbf{H}}_2^H \end{bmatrix}\right), \end{aligned} \quad (9)$$

where $\mathbf{\Gamma}_{\underline{\mathbf{y}}\underline{\mathbf{y}}}$ is the augmented covariance matrix from (2). For the special case where \mathbf{y} is a proper random vector (i.e. $\mathbf{C}_{\mathbf{y}\mathbf{y}} = \mathbf{0}$), and \mathbf{y} and \mathbf{x} are jointly proper random vectors (i.e. $\mathbf{C}_{\mathbf{x}\mathbf{y}} = \mathbf{C}_{\mathbf{y}\mathbf{x}} = \mathbf{0}$), it can be shown that (5), (6), and (7) are reduced to $\hat{\mathbf{H}}_1 = \mathbf{\Gamma}_{\mathbf{x}\mathbf{y}}\mathbf{\Gamma}_{\mathbf{y}\mathbf{y}}^{-1}$, $\hat{\mathbf{H}}_2 = \mathbf{0}$, and $\mathbf{P}_{\mathbf{y}\mathbf{y}} = \mathbf{\Gamma}_{\mathbf{y}\mathbf{y}}$, respectively. By substituting these values in (8), we obtain that in this proper case, the WLMMSE estimator from (8)

is reduced to the common LMMSE estimator for zero-mean vectors \mathbf{x} and \mathbf{y} [34]:

$$\hat{\mathbf{x}}^{\text{LMMSE}} \triangleq \mathbf{\Gamma}_{\mathbf{x}\mathbf{y}} \mathbf{\Gamma}_{\mathbf{y}\mathbf{y}}^{-1} \mathbf{y}. \quad (10)$$

The MSE of the LMMSE estimator from (10) is

$$\varepsilon_L^2 \triangleq \mathbb{E}[\|\hat{\mathbf{x}}^{\text{LMMSE}} - \mathbf{x}\|^2] = \text{tr}(\mathbf{\Gamma}_{\mathbf{x}\mathbf{x}} - \mathbf{\Gamma}_{\mathbf{x}\mathbf{y}} \mathbf{\Gamma}_{\mathbf{y}\mathbf{y}}^{-1} \mathbf{\Gamma}_{\mathbf{x}\mathbf{y}}^H). \quad (11)$$

It is shown in [19] that the difference between the MSE of the LMMSE estimator and the MSE of the WLMSE estimator is given by

$$\varepsilon_L^2 - \varepsilon_{WL}^2 = \text{tr}(\hat{\mathbf{H}}_2 \mathbf{P}_{\mathbf{y}\mathbf{y}}^* \hat{\mathbf{H}}_2^H), \quad (12)$$

which is always nonnegative as the Schur complement matrix, $\mathbf{P}_{\mathbf{y}\mathbf{y}}$, is a positive-definite matrix. Thus, there is always a gain in performing WLMSE estimation over LMMSE estimation for improper random vectors [19]. The LMMSE estimator for a proper random vector can be interpreted as ‘‘one channel processing’’ operating on \mathbf{y} only. The WLMSE estimator is ‘‘two channels processing’’ operating on \mathbf{y} via \mathbf{H}_1 and, in parallel, on \mathbf{y}_2 via \mathbf{H}_2 [20]. In this paper, we consider ‘‘two channels processing’’ in the graph frequency domain.

B. Graph Signal Processing (GSP)

Consider an undirected, connected, weighted graph $\mathcal{G}(\mathcal{V}, \mathcal{E}, \mathbf{W})$, where \mathcal{V} is the set of vertices and \mathcal{E} is the set of edges, and the $N \times N$ real-valued matrix \mathbf{W} is the nonnegative weighted adjacency matrix of the graph, where $N = |\mathcal{V}|$ is the number of vertices. The entry $\mathbf{W}_{i,j} \neq 0$ if there is an edge between node i and node j ; otherwise $\mathbf{W}_{i,j} = 0$. The Laplacian matrix of the graph is defined as

$$\mathbf{L} = \text{diag}(\mathbf{W}\mathbf{1}) - \mathbf{W}. \quad (13)$$

Since the Laplacian matrix is symmetric and semi-positive definite then its eigenvalue decomposition is given by

$$\mathbf{L} = \mathbf{V} \text{diag}(\boldsymbol{\lambda}) \mathbf{V}^{-1}, \quad (14)$$

where $\boldsymbol{\lambda}$ is an $N \times 1$ vector with the ordered eigenvalues of \mathbf{L} , $0 = \lambda_1 \leq \lambda_2 \leq \dots \leq \lambda_N$, \mathbf{V} is an $N \times N$ unitary matrix ($\mathbf{V}^{-1} = \mathbf{V}^T$), where its n th column is \mathbf{v}_n , which is the n th *real-valued* eigenvector associated with the n th eigenvalue, λ_n . A graph signal is an N -dimensional vector \mathbf{y} that assigns a scalar value to each vertex in the graph, that is, y_n is the signal value at vertex n , $n = 1, 2, \dots, N$. The graph Fourier transform (GFT) of the graph signal \mathbf{y} is defined as

$$\bar{\mathbf{y}} = \mathbf{V}^T \mathbf{y} \quad (15)$$

and the inverse GFT is given by $\mathbf{y} = \mathbf{V} \bar{\mathbf{y}}$.

Linear and shift-invariant graph filters with respect to graph shift operators (GSOs) generalize linear time-invariant filters used in time series. Let the GSO be the Laplacian matrix \mathbf{L} . A graph filter applied to the GSO is given by

$$\mathbf{F}(\mathbf{L}) = \mathbf{V} \text{diag}(\mathbf{f}(\boldsymbol{\lambda})) \mathbf{V}^T, \quad (16)$$

where $\mathbf{f}(\boldsymbol{\lambda}) = (f(\lambda_1), f(\lambda_2), \dots, f(\lambda_N))^T$, in which $f(\lambda)$ is the filter graph frequency response at graph frequency λ .

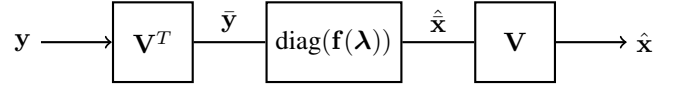


Fig. 1: GSP linear estimator (19)

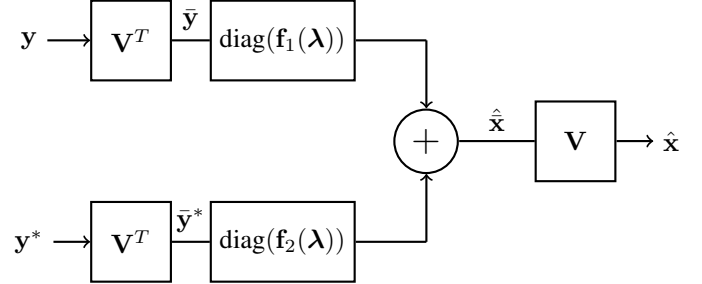


Fig. 2: Widely-linear GSP estimator (20)

C. GSP-LMMSE Estimator

The GSP-LMMSE estimator for graph signals was proposed in [6] for real-valued random vectors, and is based on diagonal covariance matrices. Similar to the derivations in [6], it can be shown that for zero-mean complex-valued random vectors \mathbf{x} and \mathbf{y} , the GSP-LMMSE estimator is given by

$$\hat{\mathbf{x}}^{(\text{GSP-LMMSE})} = \mathbf{V} \mathbf{D}_{\bar{\mathbf{x}}\bar{\mathbf{y}}}^{\mathbf{\Gamma}} (\mathbf{D}_{\bar{\mathbf{y}}\bar{\mathbf{y}}}^{\mathbf{\Gamma}})^{-1} \bar{\mathbf{y}}, \quad (17)$$

where

$$\mathbf{D}_{\bar{\mathbf{x}}\bar{\mathbf{y}}}^{\mathbf{\Gamma}} \triangleq \text{ddiag}(\mathbf{\Gamma}_{\bar{\mathbf{x}}\bar{\mathbf{y}}}), \quad \mathbf{D}_{\bar{\mathbf{y}}\bar{\mathbf{y}}}^{\mathbf{\Gamma}} \triangleq \text{ddiag}(\mathbf{\Gamma}_{\bar{\mathbf{y}}\bar{\mathbf{y}}}). \quad (18)$$

It should be noted that $\mathbf{D}_{\bar{\mathbf{y}}\bar{\mathbf{y}}}^{\mathbf{\Gamma}}$ is a real diagonal matrix. Thus, in the following, we will use $(\mathbf{D}_{\bar{\mathbf{y}}\bar{\mathbf{y}}}^{\mathbf{\Gamma}})^H = \mathbf{D}_{\bar{\mathbf{y}}\bar{\mathbf{y}}}^{\mathbf{\Gamma}}$. The GSP-LMMSE estimator in (17) minimizes the MSE among estimators that are represented as an output of a graph filter, i.e. estimators of the form (see Fig. 1)

$$\hat{\mathbf{x}} = \mathbf{V} \text{diag}(\mathbf{f}(\boldsymbol{\lambda})) \mathbf{V}^T \mathbf{y}. \quad (19)$$

The GSP-LMMSE estimator from (17) is based on the *diagonal* of the covariance matrices of the signals in the graph frequency domain $\bar{\mathbf{x}}$ and $\bar{\mathbf{y}}$ that are defined in (18). Thus, it has advantages from a computational point of view, compared with the LMMSE estimator in (10) that uses the full covariance matrices of \mathbf{x} and \mathbf{y} , and does not require inverting large, full matrices. The GSP-LMMSE estimator is, in fact, the diagonal-LMMSE estimator [35] in the *graph frequency domain*. This estimator minimizes the MSE among the linear estimators of $\bar{\mathbf{x}}$, where the estimation matrix that multiplies $\bar{\mathbf{y}}$ is restricted to be a diagonal matrix. The advantages of the GSP-LMMSE estimator and its robustness to topology changes were discussed in [6]. However, the GSP-LMMSE estimator was developed for real-valued signals, and thus does not utilize the theory of augmented complex statistics [14], [21]. In the following, we propose widely-linear estimation integrated with GSP tools.

III. WLMSE FOR GRAPH SIGNALS

In this section, the concept of widely-linear estimation is applied to the case of improper graph signals. In Subsection

III-A, we develop the GSP-WLMMSE estimator for improper graph signals. In Subsection III-B, we discuss the performance and the computational complexities of the estimators.

A. GSP-WLMMSE Estimator

In this subsection, we develop the GSP-WLMMSE estimator for a general improper complex-valued random vector. The idea of the proposed GSP-WLMMSE estimator is to generalize the ‘‘one-channel processing’’ of the GSP-LMMSE estimator operating on \mathbf{y} from Subsection II-C to ‘‘two-channels processing’’ operating on both \mathbf{y} and \mathbf{y}^* , where these two channels are in the form of an output of two graph filters.

To this end, we consider widely-linear GSP estimators that have the form (see Fig. 2)

$$\begin{aligned}\hat{\mathbf{x}} &= \mathbf{V} \text{diag}(\mathbf{f}_1(\boldsymbol{\lambda})) \mathbf{V}^T \mathbf{y} + \mathbf{V} \text{diag}(\mathbf{f}_2(\boldsymbol{\lambda})) \mathbf{V}^T \mathbf{y}^* \\ &= \mathbf{V} \text{diag}(\mathbf{f}_1(\boldsymbol{\lambda})) \bar{\mathbf{y}} + \mathbf{V} \text{diag}(\mathbf{f}_2(\boldsymbol{\lambda})) \bar{\mathbf{y}}^*,\end{aligned}\quad (20)$$

where $\bar{\mathbf{y}}$ and $\bar{\mathbf{y}}^*$ are the GFTs of \mathbf{y} and \mathbf{y}^* , respectively, as defined in (15). It can be verified that $\bar{\mathbf{y}}^* = (\bar{\mathbf{y}})^*$. We also define the matrices

$$\mathbf{D}_{\bar{\mathbf{x}}\bar{\mathbf{y}}}^{\mathbf{C}} \triangleq \text{ddiag}(\mathbf{C}_{\bar{\mathbf{x}}\bar{\mathbf{y}}}), \quad \mathbf{D}_{\bar{\mathbf{y}}\bar{\mathbf{y}}}^{\mathbf{C}} \triangleq \text{ddiag}(\mathbf{C}_{\bar{\mathbf{y}}\bar{\mathbf{y}}}).\quad (21)$$

It should be noted that the description of the diagonal covariance matrices in (18) and (21) is for the sake of notation simplicity. In practice, there is no need to compute the full covariance matrices and then take the diagonal, and only the diagonal elements should be computed. For example, in order to compute $\mathbf{D}_{\bar{\mathbf{x}}\bar{\mathbf{y}}}^{\mathbf{C}}$, one only needs to compute N elements: $\mathbb{E}[\bar{x}_n \bar{y}_n]$, $n = 1, \dots, N$. We also define

$$\rho_n \triangleq \frac{|[\mathbf{C}_{\bar{\mathbf{y}}\bar{\mathbf{y}}}]_{n,n}|^2}{|[\boldsymbol{\Gamma}_{\bar{\mathbf{y}}\bar{\mathbf{y}}}]_{n,n}|^2} = \frac{|[\mathbf{D}_{\bar{\mathbf{y}}\bar{\mathbf{y}}}^{\mathbf{C}}]_{n,n}|^2}{|[\mathbf{D}_{\bar{\mathbf{y}}\bar{\mathbf{y}}}^{\boldsymbol{\Gamma}}]_{n,n}|^2}, \quad n = 1, \dots, N.\quad (22)$$

It can be seen that the parameter ρ_n is a measure of the impropriety of the random variable \bar{y}_n . In particular, if $\bar{\mathbf{y}}$ is a proper vector then $\rho_n = 0$, $n = 1, \dots, N$.

The following theorem describes the GSP-WLMMSE estimator for a general improper model.

Theorem 1. *Let us assume that $\mathbf{C}_{\mathbf{y}\mathbf{y}} \neq \mathbf{0}$ and $\rho_n \neq 1$, $n = 1, \dots, N$. Then, the GSP-WLMMSE estimator, which is the estimator that achieves the minimum MSE within the class of widely-linear GSP estimators with the form (20), for zero-mean complex graph signals, is given by*

$$\begin{aligned}\hat{\mathbf{x}}^{(\text{GSP-WLMMSE})} &= \mathbf{V} (\mathbf{R} \mathbf{D}_{\bar{\mathbf{x}}\bar{\mathbf{y}}}^{\boldsymbol{\Gamma}} (\mathbf{D}_{\bar{\mathbf{y}}\bar{\mathbf{y}}}^{\boldsymbol{\Gamma}})^{-1} + (\mathbf{I} - \mathbf{R}) \mathbf{D}_{\bar{\mathbf{y}}\bar{\mathbf{x}}}^{\mathbf{C}} (\mathbf{D}_{\bar{\mathbf{y}}\bar{\mathbf{y}}}^{\mathbf{C}})^{-1}) \bar{\mathbf{y}} \\ &\quad + \mathbf{V} (\mathbf{R} \mathbf{D}_{\bar{\mathbf{y}}\bar{\mathbf{x}}}^{\mathbf{C}} (\mathbf{D}_{\bar{\mathbf{y}}\bar{\mathbf{y}}}^{\boldsymbol{\Gamma}})^{-1} + (\mathbf{I} - \mathbf{R}) \mathbf{D}_{\bar{\mathbf{x}}\bar{\mathbf{y}}}^{\boldsymbol{\Gamma}} ((\mathbf{D}_{\bar{\mathbf{y}}\bar{\mathbf{y}}}^{\mathbf{C}})^{-1})^*) \bar{\mathbf{y}}^*,\end{aligned}\quad (23)$$

where the diagonal coefficient matrix is

$$\mathbf{R} \triangleq \text{diag} \left(\left[\frac{1}{1 - \rho_1}, \frac{1}{1 - \rho_2}, \dots, \frac{1}{1 - \rho_N} \right] \right).\quad (24)$$

Proof: The proof appears in Appendix A. \blacksquare

It is also shown in Appendix A that under the conditions of Theorem 1, except for the condition that $\mathbf{C}_{\mathbf{y}\mathbf{y}} \neq \mathbf{0}$, the GSP-WLMMSE estimator from (23) can be written as

$$\begin{aligned}\hat{\mathbf{x}}^{(\text{GSP-WLMMSE})} &= \mathbf{V} (\mathbf{D}_{\bar{\mathbf{x}}\bar{\mathbf{y}}}^{\boldsymbol{\Gamma}} - \mathbf{D}_{\bar{\mathbf{x}}\bar{\mathbf{y}}}^{\mathbf{C}} (\mathbf{D}_{\bar{\mathbf{y}}\bar{\mathbf{y}}}^{\boldsymbol{\Gamma}})^{-1} (\mathbf{D}_{\bar{\mathbf{y}}\bar{\mathbf{y}}}^{\mathbf{C}})^*) (\mathbf{D}_{\bar{\mathbf{y}}\bar{\mathbf{y}}}^{\mathbf{P}})^{-1} \bar{\mathbf{y}} \\ &\quad + \mathbf{V} ((\mathbf{D}_{\bar{\mathbf{y}}\bar{\mathbf{x}}}^{\mathbf{C}} - \mathbf{D}_{\bar{\mathbf{y}}\bar{\mathbf{y}}}^{\mathbf{C}} (\mathbf{D}_{\bar{\mathbf{y}}\bar{\mathbf{y}}}^{\boldsymbol{\Gamma}})^{-1} (\mathbf{D}_{\bar{\mathbf{y}}\bar{\mathbf{x}}}^{\boldsymbol{\Gamma}})^*) (\mathbf{D}_{\bar{\mathbf{y}}\bar{\mathbf{y}}}^{\mathbf{P}})^{-1} \bar{\mathbf{y}}^*,\end{aligned}\quad (25)$$

where the Schur complement $\mathbf{D}_{\bar{\mathbf{y}}\bar{\mathbf{y}}}^{\mathbf{P}}$ is defined as

$$\mathbf{D}_{\bar{\mathbf{y}}\bar{\mathbf{y}}}^{\mathbf{P}} \triangleq \mathbf{D}_{\bar{\mathbf{y}}\bar{\mathbf{y}}}^{\boldsymbol{\Gamma}} - \mathbf{D}_{\bar{\mathbf{y}}\bar{\mathbf{y}}}^{\mathbf{C}} (\mathbf{D}_{\bar{\mathbf{y}}\bar{\mathbf{y}}}^{\boldsymbol{\Gamma}})^{-1} (\mathbf{D}_{\bar{\mathbf{y}}\bar{\mathbf{y}}}^{\mathbf{C}})^*.\quad (26)$$

Remark. The Schur complement matrix $\mathbf{D}_{\bar{\mathbf{y}}\bar{\mathbf{y}}}^{\mathbf{P}}$ is a diagonal matrix with non-negative values on its diagonal. Since we assume in this paper that $\boldsymbol{\Gamma}_{\mathbf{y}\mathbf{y}}$ is a non-singular matrix, $\mathbf{D}_{\bar{\mathbf{y}}\bar{\mathbf{y}}}^{\mathbf{P}}$ can also be written as

$$\mathbf{D}_{\bar{\mathbf{y}}\bar{\mathbf{y}}}^{\mathbf{P}} = \mathbf{D}_{\bar{\mathbf{y}}\bar{\mathbf{y}}}^{\boldsymbol{\Gamma}} (\mathbf{I} - (\mathbf{D}_{\bar{\mathbf{y}}\bar{\mathbf{y}}}^{\boldsymbol{\Gamma}})^{-1} \mathbf{D}_{\bar{\mathbf{y}}\bar{\mathbf{y}}}^{\mathbf{C}} (\mathbf{D}_{\bar{\mathbf{y}}\bar{\mathbf{y}}}^{\boldsymbol{\Gamma}})^{-1} (\mathbf{D}_{\bar{\mathbf{y}}\bar{\mathbf{y}}}^{\mathbf{C}})^*)^{-1} (\mathbf{D}_{\bar{\mathbf{y}}\bar{\mathbf{y}}}^{\mathbf{C}})^*).\quad (27)$$

Observe that $(\mathbf{D}_{\bar{\mathbf{y}}\bar{\mathbf{y}}}^{\boldsymbol{\Gamma}})^{-1} \mathbf{D}_{\bar{\mathbf{y}}\bar{\mathbf{y}}}^{\mathbf{C}} (\mathbf{D}_{\bar{\mathbf{y}}\bar{\mathbf{y}}}^{\boldsymbol{\Gamma}})^{-1} (\mathbf{D}_{\bar{\mathbf{y}}\bar{\mathbf{y}}}^{\mathbf{C}})^*$ is a diagonal matrix with the (n, n) th entry on its main diagonal given as ρ_n , $n = 1, 2, \dots, N$. Hence, the Schur complement matrix can also be expressed as a product of two diagonal matrices: $\mathbf{D}_{\bar{\mathbf{y}}\bar{\mathbf{y}}}^{\mathbf{P}} = \mathbf{D}_{\bar{\mathbf{y}}\bar{\mathbf{y}}}^{\boldsymbol{\Gamma}} \mathbf{R}^{-1}$.

It is also shown in Appendix A that the optimal graph filters, i.e. the graph filters that, when substituted into (20), will lead to the the GSP-WLMMSE estimator from (25), $\hat{\mathbf{x}}^{(\text{GSP-WLMMSE})}$, are

$$\hat{\mathbf{f}}_1(\boldsymbol{\lambda}) = (\mathbf{D}_{\bar{\mathbf{y}}\bar{\mathbf{y}}}^{\mathbf{P}})^{-1} ((\mathbf{d}_{\bar{\mathbf{y}}\bar{\mathbf{x}}}^{\boldsymbol{\Gamma}})^* - (\mathbf{D}_{\bar{\mathbf{y}}\bar{\mathbf{y}}}^{\mathbf{C}})^* (\mathbf{D}_{\bar{\mathbf{y}}\bar{\mathbf{y}}}^{\boldsymbol{\Gamma}})^{-1} \mathbf{d}_{\bar{\mathbf{y}}\bar{\mathbf{x}}}^{\mathbf{C}}) \quad (28)$$

and

$$\hat{\mathbf{f}}_2(\boldsymbol{\lambda}) = (\mathbf{D}_{\bar{\mathbf{y}}\bar{\mathbf{y}}}^{\mathbf{P}})^{-1} ((\mathbf{d}_{\bar{\mathbf{y}}\bar{\mathbf{x}}}^{\mathbf{C}} - \mathbf{D}_{\bar{\mathbf{y}}\bar{\mathbf{y}}}^{\mathbf{C}} (\mathbf{D}_{\bar{\mathbf{y}}\bar{\mathbf{y}}}^{\boldsymbol{\Gamma}})^{-1} (\mathbf{d}_{\bar{\mathbf{y}}\bar{\mathbf{x}}}^{\boldsymbol{\Gamma}})^*), \quad (29)$$

where $\mathbf{d}_{\bar{\mathbf{y}}\bar{\mathbf{x}}}^{\mathbf{C}} \triangleq \text{diag}(\mathbf{C}_{\bar{\mathbf{y}}\bar{\mathbf{x}}})$ and $\mathbf{d}_{\bar{\mathbf{y}}\bar{\mathbf{x}}}^{\boldsymbol{\Gamma}} \triangleq \text{diag}(\mathbf{C}_{\bar{\mathbf{y}}\bar{\mathbf{x}}})$, and $\mathbf{D}_{\bar{\mathbf{y}}\bar{\mathbf{y}}}^{\boldsymbol{\Gamma}}$ and $\mathbf{D}_{\bar{\mathbf{y}}\bar{\mathbf{y}}}^{\mathbf{C}}$ are defined in (18) and (21), respectively.

The advantages of the form in (25) compared with the form in (23) is that it also holds for $\mathbf{C}_{\mathbf{y}\mathbf{y}} = \mathbf{0}$, and that its form is reminiscent of the classical WLMMSE estimator in (8). The form in (23) enables tractable analysis of special cases and demonstrates the influence of the impropriety parameter ρ_n , $n = 1, \dots, N$.

B. Discussion: Performance and Complexity

1) *Orthogonality principle:* The WLMMSE estimator satisfies the orthogonality principle [19], which states that

$$(\hat{\mathbf{x}}^{(\text{WLMMSE})} - \mathbf{x}) \perp \mathbf{y} \quad \text{and} \quad (\hat{\mathbf{x}}^{(\text{WLMMSE})} - \mathbf{x}) \perp \mathbf{y}^*.$$

Similarly, in Appendix B it is shown that

$$(\hat{\mathbf{x}}^{(\text{GSP-WLMMSE})} - \mathbf{x}) \perp \mathbf{y} \quad \text{and} \quad (\hat{\mathbf{x}}^{(\text{GSP-WLMMSE})} - \mathbf{x}) \perp \mathbf{y}^*.$$

In other words, the estimation error vector of the GSP-WLMMSE estimator is orthogonal to both \mathbf{y} and \mathbf{y}^* .

2) *Performance:* The general form of the widely-linear GSP estimators in (20) includes the GSP-LMMSE estimator in (17) as a special case. Thus, since the GSP-WLMMSE estimator has the lowest MSE among all estimators of the form in (20), we can conclude that the MSE of the GSP-WLMMSE estimator is always lower than or equal to the MSE of the GSP-LMMSE estimator. The following theorem gives a closed-form expression for the gap in the MSE of these two estimators.

Theorem 2. *Let the trace of the MSE of the GSP-LMMSE estimator and the trace of the MSE of the GSP-WLMMSE estimator be denoted by $\varepsilon_{\text{GSP-L}}^2$ and $\varepsilon_{\text{GSP-WL}}^2$, respectively. Then, the difference between the trace MSEs is*

$$\varepsilon_{\text{GSP-L}}^2 - \varepsilon_{\text{GSP-WL}}^2 = \hat{\mathbf{f}}_2^H(\boldsymbol{\lambda}) \mathbf{D}_{\bar{\mathbf{y}}\bar{\mathbf{y}}}^{\mathbf{P}} \hat{\mathbf{f}}_2(\boldsymbol{\lambda}), \quad (30)$$

where $\mathbf{D}_{\hat{\mathbf{y}}\hat{\mathbf{y}}}^{\mathbf{P}}$ and $\hat{\mathbf{f}}_2(\boldsymbol{\lambda})$ are given in (26) and (29), respectively.

Proof: The proof appears in Appendix C. ■

Since the Schur complement $\mathbf{D}_{\hat{\mathbf{y}}\hat{\mathbf{y}}}^{\mathbf{P}}$ is a positive-definite matrix, the quadratic form in (30) is always nonnegative, that is, $\varepsilon_{GSP-L}^2 - \varepsilon_{GSP-WL}^2 \geq 0$. In other words, the trace of the MSE of the GSP-LMMSE estimator is always larger than or equal to the trace of the MSE of the GSP-WLMMSE estimator. Thus, in the case of improper graph signals, there is a performance gain in GSP-WLMMSE estimation over GSP-LMMSE estimation. It should be noted that since the GSP-WLMMSE belongs to the family of widely-linear estimators, it achieves an intermediate performance between the optimal widely-linear filter (WLMMSE estimator) and the optimal linear filter in the graph domain (GSP-LMMSE estimator).

3) *Computational complexity:* In terms of computational complexity, the WLMMSE estimator from (8) requires: 1) computing the inverse of the $N \times N$ complex-valued matrices $\Gamma_{\mathbf{y}\mathbf{y}}$ and $\mathbf{P}_{\mathbf{y}\mathbf{y}}$, which has a complexity of $\mathcal{O}(N^3)$; and 2) performing full matrix multiplications, with a computational complexity of $\mathcal{O}(N^3)$. The GSP-WLMMSE estimator from (23) requires: 1) computing the inverse of the diagonal matrices $\mathbf{D}_{\hat{\mathbf{y}}\hat{\mathbf{y}}}^{\mathbf{F}}$ and $\mathbf{D}_{\hat{\mathbf{y}}\hat{\mathbf{y}}}^{\mathbf{C}}$, which has a complexity of $\mathcal{O}(N)$; and 2) performing multiplications of diagonal matrices with a cost of $\mathcal{O}(N^2)$. However, the use of the graph frequency domain in the GSP-WLMMSE estimator requires the computation of the eigenvalue decomposition (EVD) of the Laplacian matrix, which is of order $\mathcal{O}(N^3)$. This computation can be performed offline, e.g. by low-complexity methods [36]. Alternatively, the graph filters can be replaced by specific parametrization and local implementations.

4) *Implementation with sample covariance values:* The recovery of random graph signals by the discussed linear and widely-linear estimators can be used when the second-order statistics are completely specified. However, for general non-linear models, the covariance matrices of the graph signal and the observations do not have closed-form expressions. In these cases, we can use data to estimate the second-order statistics and then recover the graph signals based on the estimated statistics. That is, assume that we have data (we can always generate such data for a given model) which is comprised of a training set consisting of K pairs of the zero-mean inputs and their corresponding zero-mean measurements, denoted by $\mathcal{D} = \{\mathbf{x}_k, \mathbf{y}_k\}_{k=1}^K$. Then, the sample cross-covariance and the sample complementary cross-covariance matrices are

$$\hat{\mathbf{\Gamma}}_{\mathbf{x}\mathbf{y}} = \frac{1}{K} \sum_{k=1}^K \mathbf{x}_k \mathbf{y}_k^H \quad \text{and} \quad \hat{\mathbf{C}}_{\mathbf{x}\mathbf{y}} = \frac{1}{K} \sum_{k=1}^K \mathbf{x}_k \mathbf{y}_k^T. \quad (31)$$

Similarly, we can calculate all the other sample diagonal and non-diagonal covariance matrices that are needed for the estimators. The sample versions of the LMMSE, WLMMSE, GSP-LMMSE, and GSP-WLMMSE estimators, that are obtained by plugging the sample covariance matrices into the original estimators, can be used (see, e.g. regarding the sample LMMSE estimator in [37] and p. 728 in [38], and regarding the sample GSP-LMMSE estimator in [6]).

However, in many practical applications, the graph signal has a broad correlation function, so that estimating the covariance matrices from data with high accuracy necessitates a larger

sample size than is available. In particular, in settings where the sample size of the training data used to compute the sample-mean versions (K) is comparable to the observation dimension (N), the sample-LMMSE and sample-WLMMSE estimators exhibit severe performance degradation [39]. This is because the sample covariance matrix is not well-conditioned in the small sample size regime, and inverting it amplifies the estimation error. In such cases, the sample-GSP-LMMSE estimator and the sample-GSP-WLMMSE estimator have a huge advantage, since they require the estimation of only two and four (respectively) N -length vectors that contain the diagonal of the covariance and of the cross-covariance matrices from (18) and (21). This is in contrast to the sample-LMMSE and sample-WLMMSE estimators that require estimating two and four (respectively) full $N \times N$ matrices. This advantage improves the sample-GSP-WLMMSE estimator performance compared to the sample-WLMMSE estimator, with limited datasets used for the non-parametric estimation of the different sample-covariance matrices. Moreover, the estimation of the inverse sample diagonal covariance matrices, $(\mathbf{D}_{\hat{\mathbf{y}}\hat{\mathbf{y}}}^{\mathbf{F}})^{-1}$ and $(\mathbf{D}_{\hat{\mathbf{y}}\hat{\mathbf{y}}}^{\mathbf{C}})^{-1}$ from (23), is more robust to limited data than the estimation of the inverse of the full sample covariance matrices, required by the sample-WLMMSE estimator.

IV. SPECIAL CASES AND RELATION WITH EXISTING ESTIMATORS

In this section, we investigate the properties of the proposed GSP-WLMMSE estimator for the important special cases of proper signal and data (Subsection IV-A), maximal improper observation vectors (Subsection IV-B), and real-valued unknown graph signals (Subsection IV-C). In addition, we discuss the relations between the GSP-WLMMSE estimator and the scalar widely-linear estimators (Subsection IV-D), and the conventional WLMMSE estimator (Subsection IV-E).

A. Proper case

This case is well known in the literature, and considered to be the normal case. Let us assume that:

- C.1) The signal and measurement are cross-proper, i.e. $\mathbf{C}_{\mathbf{y}\mathbf{x}} = \mathbf{0}$;
- C.2) The measurement vector \mathbf{y} is proper, i.e. $\mathbf{C}_{\mathbf{y}\mathbf{y}} = \mathbf{0}$.

Condition C.1 implies that $\mathbf{D}_{\hat{\mathbf{y}}\hat{\mathbf{x}}}^{\mathbf{C}} = \mathbf{0}$. By substituting Condition C.2 in (22)-(24), we obtain that $\rho_n = 0, \forall n = 1, \dots, N$, and $\mathbf{R} = \mathbf{I}$. By substituting $\mathbf{R} = \mathbf{I}$ and $\mathbf{D}_{\hat{\mathbf{y}}\hat{\mathbf{x}}}^{\mathbf{C}} = \mathbf{0}$ in (23), one obtains that in the proper case, the GSP-WLMMSE estimator is reduced to the GSP-LMMSE estimator from (17). Thus, in the proper case, there is no gain from using the GSP-WLMMSE estimator over the GSP-LMMSE estimator.

In contrast, if we only assumed that Condition C.2 holds, i.e. $\mathbf{C}_{\mathbf{y}\mathbf{y}} = \mathbf{0}$, and no specific assumption is introduced for the estimand \mathbf{x} , then (23) is reduced to

$$\hat{\mathbf{x}}^{(\text{GSP-WLMMSE})} = \hat{\mathbf{x}}^{(\text{GSP-LMMSE})} + \mathbf{V} \mathbf{D}_{\hat{\mathbf{y}}\hat{\mathbf{x}}}^{\mathbf{C}} (\mathbf{D}_{\hat{\mathbf{y}}\hat{\mathbf{y}}}^{\mathbf{F}})^{-1} \hat{\mathbf{y}}^*, \quad (32)$$

where $\hat{\mathbf{x}}^{(\text{GSP-LMMSE})}$ is given in (17). Thus, in this case the GSP-WLMMSE estimator is different from the GSP-LMMSE estimator and a performance gain can be obtained. The structure of the GSP-WLMMSE estimator in this case can be explained by noting that the circularity assumption implies

that the vectors \mathbf{y} and \mathbf{y}^* are uncorrelated. Thus, the Hilbert subspaces generated by these vectors are orthogonal, and taking into account \mathbf{y}^* does not change the term coming from \mathbf{y} only. Thus, a nonzero matrix $\mathbf{C}_{\mathbf{y}\mathbf{x}}$ necessarily implies an increment of the estimation performance when using widely-linear estimators instead of linear estimators. This result is an extension of the results in [19] for the WLM MSE estimator.

B. Maximal improper case

Let \mathbf{F} be a deterministic $N \times N$ complex-valued unitary matrix, $\mathbf{F}^H \mathbf{F} = \mathbf{F} \mathbf{F}^H = \mathbf{I}$. Then, if the measurement vector \mathbf{y} is maximally improper [40], i.e. $\mathbf{y} = \mathbf{F} \mathbf{y}^*$ with probability 1, we obtain that $\mathbf{\Gamma}_{\mathbf{y}\mathbf{y}} = \mathbb{E}[\mathbf{y}\mathbf{y}^T \mathbf{F}^H] = \mathbf{C}_{\mathbf{y}\mathbf{y}} \mathbf{F}^H$ and $\mathbf{\Gamma}_{\mathbf{x}\mathbf{y}} = \mathbb{E}[\mathbf{x}\mathbf{y}^T \mathbf{F}^H] = \mathbf{C}_{\mathbf{x}\mathbf{y}} \mathbf{F}^H$. Thus, if, in addition, \mathbf{F} is a diagonal matrix, then, according to (22), $\rho_n = 1$ for any $n = 1, \dots, N$. Thus, Theorem 1, which was developed under the assumption that $\rho_n \neq 1$, does not hold. In this case, it can be shown (similar to the derivations in Appendix A) that the GSP-WLM MSE estimator is reduced to the GSP-LMMSE estimator from (17). Thus, for a maximal improper \mathbf{y} with a diagonal matrix \mathbf{F} , we obtain that the GSP-WLM MSE estimator coincides with the GSP-LMMSE estimator (irrespective of whether or not \mathbf{x} is proper). This is similar to the property for the WLM MSE estimator and the LMMSE estimator [41]. However, if \mathbf{F} is not a diagonal matrix, then the GSP-WLM MSE estimator is different from the GSP-LMMSE estimator. This is in contrast to the results for the WLM MSE and LMMSE for non-graph signals (see in [41] after Eq. (46)). This can be explained by the fact that, while $\bar{\mathbf{y}}$ and $\bar{\mathbf{y}}^*$ carry the same second-order information about \mathbf{x} where \mathbf{y} is maximally improper (i.e. $\mathbf{y} = \mathbf{F} \mathbf{y}^*$), the GSP estimators only use the diagonal of the second-order information, which may be different for $\mathbf{F} \mathbf{y}^*$ and \mathbf{y}^* . Thus, the limitation to outputs of graph filters (or, equivalently, to diagonal covariance matrices in the graph frequency domain) changes the information that we can obtain from $\bar{\mathbf{y}}$ and $\bar{\mathbf{y}}^*$ for cases where \mathbf{F} is a non-diagonal unitary matrix. In fact, even for the real-value case described in Subsection II-C, if we minimize the MSE among the estimators of the form

$$\hat{\mathbf{x}} = \mathbf{V} \text{diag}(\mathbf{f}_1(\boldsymbol{\lambda})) \mathbf{V}^T \mathbf{y} + \mathbf{V} \text{diag}(\mathbf{f}_2(\boldsymbol{\lambda})) \mathbf{V}^T \mathbf{G} \mathbf{y}, \quad (33)$$

where \mathbf{G} is a real-valued non-diagonal orthogonal matrix, $\mathbf{G}^T \mathbf{G} = \mathbf{I}$, instead of the form in (19), then we can obtain an estimator that will outperform the GSP-LMMSE estimator.

C. Real-values case

If the signal \mathbf{x} is real (but \mathbf{y} is complex), we have $\mathbf{D}_{\bar{\mathbf{y}}\bar{\mathbf{x}}}^{\mathbf{C}} = \mathbf{D}_{\bar{\mathbf{y}}\bar{\mathbf{x}}}^{\mathbf{r}} = (\mathbf{D}_{\bar{\mathbf{x}}\bar{\mathbf{y}}}^{\mathbf{r}})^*$. This leads to the simplified expression of the GSP-WLM MSE estimator from (23):

$$\hat{\mathbf{x}}^{(\text{GSP-WLM MSE})} = 2\mathbf{V} \Re \left\{ \left(\mathbf{R} \mathbf{D}_{\bar{\mathbf{x}}\bar{\mathbf{y}}}^{\mathbf{r}} (\mathbf{D}_{\bar{\mathbf{y}}\bar{\mathbf{y}}}^{\mathbf{r}})^{-1} + (\mathbf{I} - \mathbf{R}) \mathbf{D}_{\bar{\mathbf{y}}\bar{\mathbf{x}}}^{\mathbf{r}} (\mathbf{D}_{\bar{\mathbf{y}}\bar{\mathbf{y}}}^{\mathbf{C}})^{-1} \right) \bar{\mathbf{y}} \right\}. \quad (34)$$

Since \mathbf{V} is a real matrix, the GSP-WLM MSE estimator of a real graph signal \mathbf{x} in (34) is real. In contrast, the GSP-LMMSE estimator from (17) is generally complex, which may lead to absurd results.

D. Relation to scalar widely-linear estimators

In [42] it is proposed to keep a linear filter and apply scalar widely-linear operations to the components of the filter output. That is, to minimize the MSE among scalar widely-linear estimators of the form

$$\hat{\mathbf{x}} = \text{diag}(\mathbf{a}) \mathbf{G} \mathbf{y} + \text{diag}(\mathbf{b}) \mathbf{G} \mathbf{y}^*. \quad (35)$$

The total number of unknown complex coefficients is $N^2 + 2N$ for scalar widely-linear estimators in (35) (given by \mathbf{G} , \mathbf{a} , and \mathbf{b}), $2N$ for the proposed widely-linear GSP estimator of the form in (20) (given by $f_1(\boldsymbol{\lambda})$ and $f_2(\boldsymbol{\lambda})$), $2N^2$ in the case of general widely-linear estimators in the form of (3) (given by \mathbf{H}_1 and \mathbf{H}_2), and N in the case of a GSP linear estimator in the form of (19) (given by $f_1(\boldsymbol{\lambda})$). Where the number of unknowns increases, we have more degrees of freedom for each estimator, which decreases the MSE. On the other hand, this results in a more demanding computation, and may be impractical for implementation with sample-mean values, where the actual statistic is intractable (see more in Subsection III-B).

It can be seen that the GSP widely-linear estimator can be written in the graph frequency domain as

$$\hat{\mathbf{x}} = \text{diag}(\mathbf{f}_1(\boldsymbol{\lambda})) \bar{\mathbf{y}} + \text{diag}(\mathbf{f}_2(\boldsymbol{\lambda})) \bar{\mathbf{y}}^*. \quad (36)$$

Therefore, the proposed GSP widely-linear estimator can be interpreted as a scalar widely-linear estimator [42] in the *graph frequency domain* where $\mathbf{G} = \mathbf{I}$.

E. Relation with the conventional WLM MSE estimator

The following theorem states sufficient and necessary conditions for the proposed GSP-WLM MSE estimator to achieve the state-of-the-art WLM MSE estimator.

Theorem 3. *The GSP-WLM MSE estimator from Theorem 1 coincides with the WLM MSE estimator from (8) if*

$$\begin{aligned} & (\mathbf{\Gamma}_{\bar{\mathbf{x}}\bar{\mathbf{y}}} - \mathbf{C}_{\bar{\mathbf{x}}\bar{\mathbf{y}}} (\mathbf{\Gamma}_{\bar{\mathbf{y}}\bar{\mathbf{y}}}^{-1})^* \mathbf{C}_{\bar{\mathbf{y}}\bar{\mathbf{y}}}^*) \mathbf{P}_{\bar{\mathbf{y}}\bar{\mathbf{y}}}^{-1} \\ & = (\mathbf{D}_{\bar{\mathbf{x}}\bar{\mathbf{y}}}^{\mathbf{r}} - \mathbf{D}_{\bar{\mathbf{x}}\bar{\mathbf{y}}}^{\mathbf{C}} (\mathbf{D}_{\bar{\mathbf{y}}\bar{\mathbf{y}}}^{\mathbf{r}})^{-1} (\mathbf{D}_{\bar{\mathbf{y}}\bar{\mathbf{y}}}^{\mathbf{C}})^*) (\mathbf{D}_{\bar{\mathbf{y}}\bar{\mathbf{y}}}^{\mathbf{P}})^{-1} \end{aligned} \quad (37)$$

and

$$\begin{aligned} & (\mathbf{C}_{\bar{\mathbf{x}}\bar{\mathbf{y}}} - \mathbf{\Gamma}_{\bar{\mathbf{x}}\bar{\mathbf{y}}} \mathbf{\Gamma}_{\bar{\mathbf{y}}\bar{\mathbf{y}}}^{-1} \mathbf{C}_{\bar{\mathbf{y}}\bar{\mathbf{y}}}) (\mathbf{P}_{\bar{\mathbf{y}}\bar{\mathbf{y}}}^{-1})^* \\ & = ((\mathbf{D}_{\bar{\mathbf{y}}\bar{\mathbf{x}}}^{\mathbf{C}} - \mathbf{D}_{\bar{\mathbf{y}}\bar{\mathbf{y}}}^{\mathbf{C}} (\mathbf{D}_{\bar{\mathbf{y}}\bar{\mathbf{y}}}^{\mathbf{r}})^{-1})^* (\mathbf{D}_{\bar{\mathbf{y}}\bar{\mathbf{x}}}^{\mathbf{r}})^*) (\mathbf{D}_{\bar{\mathbf{y}}\bar{\mathbf{y}}}^{\mathbf{P}})^{-1}, \end{aligned} \quad (38)$$

where we assume that $\mathbf{\Gamma}_{\bar{\mathbf{y}}\bar{\mathbf{y}}}$, $\mathbf{P}_{\bar{\mathbf{y}}\bar{\mathbf{y}}}$, $\mathbf{D}_{\bar{\mathbf{y}}\bar{\mathbf{y}}}^{\mathbf{r}}$, and $\mathbf{D}_{\bar{\mathbf{y}}\bar{\mathbf{y}}}^{\mathbf{P}}$ are non-singular matrices.

Proof: By comparing (8) and (25), it can be verified that the GSP-WLM MSE estimator coincides with the WLM MSE estimator for any observation vector \mathbf{y} if the second-order statistics of \mathbf{x} and \mathbf{y} satisfy

$$\begin{aligned} & (\mathbf{\Gamma}_{\mathbf{x}\mathbf{y}} - \mathbf{C}_{\mathbf{x}\mathbf{y}} (\mathbf{\Gamma}_{\mathbf{y}\mathbf{y}}^{-1})^* \mathbf{C}_{\mathbf{y}\mathbf{y}}^*) \mathbf{P}_{\mathbf{y}\mathbf{y}}^{-1} \\ & = \mathbf{V} (\mathbf{D}_{\bar{\mathbf{x}}\bar{\mathbf{y}}}^{\mathbf{r}} - \mathbf{D}_{\bar{\mathbf{x}}\bar{\mathbf{y}}}^{\mathbf{C}} (\mathbf{D}_{\bar{\mathbf{y}}\bar{\mathbf{y}}}^{\mathbf{r}})^{-1} (\mathbf{D}_{\bar{\mathbf{y}}\bar{\mathbf{y}}}^{\mathbf{C}})^*) (\mathbf{D}_{\bar{\mathbf{y}}\bar{\mathbf{y}}}^{\mathbf{P}})^{-1} \mathbf{V}^T \end{aligned} \quad (39)$$

and

$$\begin{aligned} & (\mathbf{C}_{\mathbf{x}\mathbf{y}} - \mathbf{\Gamma}_{\mathbf{x}\mathbf{y}} \mathbf{\Gamma}_{\mathbf{y}\mathbf{y}}^{-1} \mathbf{C}_{\mathbf{y}\mathbf{y}}) (\mathbf{P}_{\mathbf{y}\mathbf{y}}^{-1})^* \\ & = \mathbf{V} ((\mathbf{D}_{\bar{\mathbf{y}}\bar{\mathbf{x}}}^{\mathbf{C}} - \mathbf{D}_{\bar{\mathbf{y}}\bar{\mathbf{y}}}^{\mathbf{C}} (\mathbf{D}_{\bar{\mathbf{y}}\bar{\mathbf{y}}}^{\mathbf{r}})^{-1})^* (\mathbf{D}_{\bar{\mathbf{y}}\bar{\mathbf{x}}}^{\mathbf{r}})^*) (\mathbf{D}_{\bar{\mathbf{y}}\bar{\mathbf{y}}}^{\mathbf{P}})^{-1}. \end{aligned} \quad (40)$$

By right and left multiplication of (39) and (40) by \mathbf{V}^T and \mathbf{V} , respectively, and using $\mathbf{V}^T \mathbf{V} = \mathbf{V} \mathbf{V}^T = \mathbf{I}$ and the GFT

definition in (15), the conditions in (39) and (40) can be rewritten as in (37) and (38), respectively. ■

A sufficient condition for (37) and (38) to hold is that the matrices $\Gamma_{\bar{y}\bar{y}}$, $\Gamma_{\bar{x}\bar{y}}$, $\mathbf{C}_{\bar{x}\bar{y}}$, $\mathbf{C}_{\bar{y}\bar{y}}$, and $\mathbf{P}_{\bar{y}\bar{y}}$ are diagonal matrices. In the following theorem we present a special case for which these matrices are diagonal, and thus, the GSP-WLMMSE estimator coincides with the WLMMSE estimator.

Theorem 4. *The GSP-WLMMSE estimator coincides with the WLMMSE estimator if the measurement vector is the output of two linear graph filters, $h_1(\cdot)$ and $h_2(\cdot)$:*

$$\mathbf{y} = \mathbf{V}h_1(\Lambda)\mathbf{V}^T\mathbf{x} + \mathbf{V}h_2(\Lambda)\mathbf{V}^T\mathbf{x}^* + \mathbf{w}, \quad (41)$$

and $\mathbf{C}_{\mathbf{x}\mathbf{x}}$ and $\Gamma_{\mathbf{x}\mathbf{x}}$ are diagonalizable by the eigenvector matrix of the Laplacian, \mathbf{V} , i.e. $\mathbf{C}_{\bar{x}\bar{x}}$ and $\Gamma_{\bar{x}\bar{x}}$ are diagonal matrices. The noise term \mathbf{w} is assumed to be a zero-mean vector that is also uncorrelated in the graph frequency domain, i.e. $\mathbf{C}_{\bar{w}\bar{w}}$ is a diagonal matrix. In addition, \mathbf{x} and \mathbf{w} are assumed to be statistically independent.

Proof: The proof is given in Appendix D. ■

An interesting case is the noiseless case where the first graph filter vanishes, i.e. $h_1(\Lambda) = \mathbf{0}$, and the measurement model from (41) is reduced to

$$\mathbf{y} = \mathbf{V}h_2(\Lambda)\mathbf{V}^T\mathbf{x}^*. \quad (42)$$

In addition, it is assumed that $h_2(\Lambda)$ is invertible such that $h_2^{-1}(\Lambda)h_2(\Lambda) = \mathbf{I}$. By substituting $\Gamma_{\bar{w}\bar{w}} = \mathbf{C}_{\bar{w}\bar{w}} = \mathbf{0}$ and $h_1(\Lambda) = \mathbf{0}$ in (83)-(87) from Appendix D, and using the fact that $(\mathbf{D}_{\bar{x}\bar{x}}^\Gamma)^* = \mathbf{D}_{\bar{x}\bar{x}}^\Gamma$, we obtain that in this case

$$\Gamma_{\bar{y}\bar{y}} = h_2(\Lambda)\Gamma_{\bar{x}\bar{x}}^*h_2^*(\Lambda) \Rightarrow \mathbf{D}_{\bar{y}\bar{y}}^\Gamma = h_2(\Lambda)\mathbf{D}_{\bar{x}\bar{x}}^\Gamma h_2^*(\Lambda), \quad (43)$$

$$\mathbf{C}_{\bar{y}\bar{y}} = h_2(\Lambda)\mathbf{C}_{\bar{x}\bar{x}}^*h_2(\Lambda) \Rightarrow \mathbf{D}_{\bar{y}\bar{y}}^C = h_2(\Lambda)(\mathbf{D}_{\bar{x}\bar{x}}^C)^*h_2(\Lambda), \quad (44)$$

$$\Gamma_{\bar{x}\bar{y}} = \mathbf{C}_{\bar{x}\bar{x}}h_2^*(\Lambda) \Rightarrow \mathbf{D}_{\bar{x}\bar{y}}^\Gamma = \mathbf{D}_{\bar{x}\bar{x}}^\Gamma h_2^*(\Lambda), \quad (45)$$

and

$$\mathbf{C}_{\bar{x}\bar{y}} = \Gamma_{\bar{x}\bar{x}}h_2(\Lambda) \Rightarrow \mathbf{D}_{\bar{x}\bar{y}}^C = \mathbf{D}_{\bar{x}\bar{x}}^C h_2(\Lambda). \quad (46)$$

By substituting (43)-(46) in (25)-(26), we obtain that in this case

$$\mathbf{D}_{\bar{y}\bar{y}}^P = h_2(\Lambda) \left(\mathbf{D}_{\bar{x}\bar{x}}^\Gamma - (\mathbf{D}_{\bar{x}\bar{x}}^C)^* (\mathbf{D}_{\bar{x}\bar{x}}^\Gamma)^{-1} \mathbf{D}_{\bar{x}\bar{x}}^C \right) h_2^*(\Lambda) \quad (47)$$

and

$$\begin{aligned} & \hat{\mathbf{x}}^{(\text{GSP-WLMMSE})} \\ &= \mathbf{V} \left(\mathbf{D}_{\bar{x}\bar{x}}^C - \mathbf{D}_{\bar{x}\bar{x}}^\Gamma (\mathbf{D}_{\bar{x}\bar{x}}^\Gamma)^{-1} \mathbf{D}_{\bar{x}\bar{x}}^C \right) h_2^*(\Lambda) (\mathbf{D}_{\bar{y}\bar{y}}^P)^{-1} \bar{\mathbf{y}} \\ & \quad + \mathbf{V}h_2(\Lambda) \left(\mathbf{D}_{\bar{x}\bar{x}}^\Gamma - (\mathbf{D}_{\bar{x}\bar{x}}^C)^* (\mathbf{D}_{\bar{x}\bar{x}}^\Gamma)^{-1} \mathbf{D}_{\bar{x}\bar{x}}^C \right) (\mathbf{D}_{\bar{y}\bar{y}}^P)^{-1} \bar{\mathbf{y}}^* \\ &= \mathbf{V}\mathbf{D}_{\bar{y}\bar{y}}^P h_2^{-1}(\Lambda) (\mathbf{D}_{\bar{y}\bar{y}}^P)^{-1} \bar{\mathbf{y}}^* = \mathbf{V}h_2^{-1}(\Lambda) \bar{\mathbf{y}}^*, \end{aligned} \quad (48)$$

where we used the fact that for any diagonal matrices with appropriate dimensions \mathbf{D}_A , \mathbf{D}_B , \mathbf{D}_C , we have $\mathbf{D}_A\mathbf{D}_B\mathbf{D}_C = \mathbf{D}_B\mathbf{D}_C\mathbf{D}_A$. By comparing (48) and (42), it can be seen that the GSP-WLMMSE estimator provides a zero-error estimation in this case.

On the other hand, by substituting (43) and (45) in (17), we obtain that the GSP-LMMSE estimator for this case is given by

$$\hat{\mathbf{x}}^{(\text{GSP-LMMSE})} = \mathbf{V}\mathbf{D}_{\bar{x}\bar{x}}^C (\mathbf{D}_{\bar{x}\bar{x}}^\Gamma)^{-1} h_2^{-1}(\Lambda) \bar{\mathbf{y}}, \quad (49)$$

$$\hat{\mathbf{x}}^{(\text{GSP-LMMSE})} = \mathbf{V}h_2(\Lambda)\mathbf{C}_{\bar{x}\bar{x}}^* (h_2^*(\Lambda))^{-1} (\Gamma_{\bar{x}\bar{x}}^*)^{-1} h_2^{-1}(\Lambda) \bar{\mathbf{y}}. \quad (50)$$

For $\mathbf{x} = \mathbf{x}^*$ (i.e. a real vector \mathbf{x}) we obtain that the GSP-LMMSE estimator coincides with the zero-error GSP-WLMMSE estimator. However, for the general case, the estimator in (49) will provide a nonzero estimation error, and thus is less attractive than the GSP-WLMMSE estimator.

V. NUMERICAL EXAMPLES

In this section, we evaluate the performance of the sample-mean versions of the LMMSE, WLMMSE, GSP-LMMSE, and GSP-WLMMSE estimators, where the covariance matrices are replaced by their sample-mean versions, as explained in Subsection III-B4. These estimators are denoted here as sLMMSE, sWLMMSE, sGSP-LMMSE, and sGSP-WLMMSE estimators. In addition, given M Monte-Carlo trials, the empirical MSE of an estimator is computed as

$$\text{MSE} = \frac{1}{M} \sum_{m=1}^M \|\hat{\mathbf{x}}_m - \mathbf{x}_m\|^2,$$

where \mathbf{x}_m is the vector at the m th trial, and $\hat{\mathbf{x}}_m$ is its estimate. In all simulations, we use $M = 10,000$.

A. Example 1: Linear graph-filter-based system

In this synthetic example, we consider a random graph with $N = 100$ nodes. The considered topology is shown in Fig. 3.

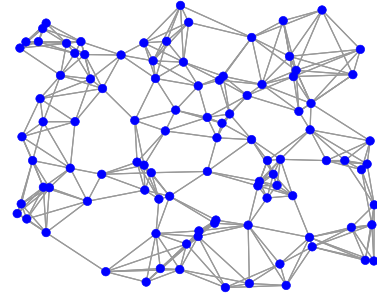


Fig. 3: The considered network of Example 1 and Example 2 with $N = 100$ sensors and an average of 350 edges.

The zero-mean input graph signal \mathbf{x} is given by [43, p. 45]:

$$\mathbf{x} = \sqrt{1 - \eta^2} \boldsymbol{\epsilon}_r + j\eta \boldsymbol{\epsilon}_i, \quad (51)$$

where $\boldsymbol{\epsilon}_r$ and $\boldsymbol{\epsilon}_i$ are two uncorrelated real-valued random processes, both Gaussian distributed with zero mean and unit variance. Thus, the covariance matrix and the complementary covariance matrix of \mathbf{x} are $\Gamma_{\mathbf{x}\mathbf{x}} = \mathbf{I}_N$ and $\mathbf{C}_{\mathbf{x}\mathbf{x}} = (1 - 2\eta^2)\mathbf{I}_N$, respectively. Hence, as the value of $\eta \in [0, 1)$ changes, the degree of non-circularity of the random vector also changes, and for $\eta = 1/\sqrt{2}$ the vector \mathbf{x} becomes circular.

The observed graph signal in this example is

$$\mathbf{y} = \mathbf{H}\mathbf{x} + \mathbf{n}, \quad (52)$$

where \mathbf{n} is a zero-mean proper Gaussian distributed graph signal with a covariance matrix $\sigma^2 \mathbf{I}_N$ that is independent of \mathbf{x} . The matrix $\mathbf{H} \in \mathbb{R}^{N \times N}$ is a graph filter given by

$$\mathbf{H} = \mathbf{V}h(\Lambda)\mathbf{V}^T, \quad (53)$$

where $h(\Lambda)$ is a diagonal matrix where the entries on the diagonals are auto-regressive moving-average (ARMA) graph filters [25] that are given by

$$h(\lambda_i) = \frac{\sum_{p=0}^{P-1} \lambda_i^p c_p}{1 + \sum_{q=1}^{Q-1} \lambda_i^q a_q}, \quad (54)$$

where $\{c_p\}_{p=0}^{P-1}$ and $\{a_q\}_{q=1}^Q$ are the filter coefficients, and P, Q are the filter orders. The theoretical covariance matrix and complementary matrix of the random vectors \mathbf{x} and \mathbf{y} are, respectively,

$$\begin{aligned} \Gamma_{\mathbf{xy}} &= \mathbf{H}^H, \quad \Gamma_{\mathbf{yy}} = \mathbf{H}\mathbf{H}^H + \sigma^2 \mathbf{I}_N, \\ \mathbf{C}_{\mathbf{xy}} &= \mathbf{C}_{\mathbf{xx}}\mathbf{H}^T, \quad \mathbf{C}_{\mathbf{yy}} = \mathbf{H}\mathbf{C}_{\mathbf{xx}}\mathbf{H}^T. \end{aligned} \quad (55)$$

These values are used to calculate the theoretical MSEs of the theoretical LMMSE, WLMME, GSP-LMMSE, and GSP-WLMME estimators (i.e. with the true statistical covariance matrices) given by the mathematical terms ε_L^2 , ε_{WL}^2 , ε_{GSP-L}^2 , and ε_{GSP-WL}^2 from (11), (9), (79), and (75), respectively. The empirical MSEs of the sample-mean versions, sLMMSE, sWLMME, sGSP-LMMSE, and sGSP-WLMME estimators, and the theoretical MSEs of the estimators (ε_L^2 , ε_{WL}^2 , ε_{GSP-L}^2 , and ε_{GSP-WL}^2) are presented in Fig. 4 for $\eta = 0.1, 0.2, 0.3, 0.4$ versus the size of the training data, K , of the sample-mean versions of the estimators (see (31)).

There are a few insights we can highlight from this experiment:

- 1) Since the MSEs of the LMMSE, WLMME, GSP-LMMSE, and GSP-WLMME estimators, given by ε_L^2 , ε_{WL}^2 , ε_{GSP-L}^2 , and ε_{GSP-WL}^2 , respectively, are based on the true, theoretical values of the covariance matrices and do not use the training data, their performance is independent of K . It can be seen that for a large enough K , the theoretical MSEs of the estimators agree with their empirical MSEs. Further, as K is small ($K < 1,000$), the MSEs of both the sLMMSE and the sWLMME estimators diverge. This occurs as the number of unknowns of both estimators is approximately N^2 , and therefore one should have $K > N^2 \approx 10,000$ to obtain a reliable non-parametric estimate of the entries of the sample covariance matrices defining the estimators.
- 2) On the other hand, as the sGSP-LMMSE and the sGSP-WLMME estimators are diagonals, we only need about $K \approx N$ to obtain reliable estimates. It is clear that both the sGSP-WLMME and the sGSP-LMMSE estimators outperform the LMMSE and WLMME estimators for all values of η and N . Still, for $K \rightarrow \infty$, this result will be reversed.
- 3) Finally, as the graph signal \mathbf{x} becomes more improper, i.e. as η decreases, the MSE of the sGSP-WLMME estimator is smaller than the MSE of the sGSP-LMMSE estimator in accordance with the theoretical study in Subsection III-B.

We also evaluated the MSE of the different estimators as a function of the non-circularity coefficient, η , for η that lies in

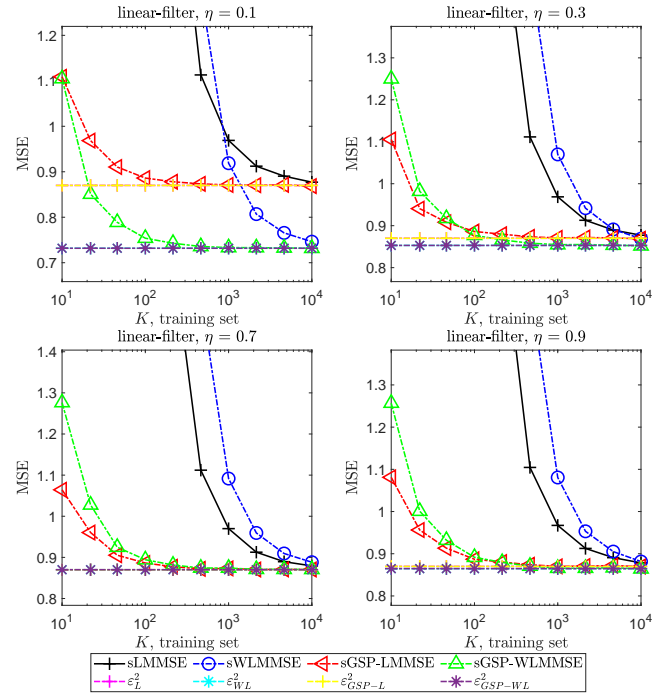


Fig. 4: The theoretical MSEs, ε_L^2 , ε_{WL}^2 , ε_{GSP-L}^2 , and ε_{GSP-WL}^2 , and the empirical MSEs of the sLMMSE, sWLMME, sGSP-LMMSE, and sGSP-WLMME estimators, for the linear system of Example 1 versus the size of the training data, K , for the non-circularity coefficient, $\eta = 0.1, 0.3, 0.7$ and 0.9 .

the interval 0 to 1, and for two values of sizes of the training data, that is, $K = 100$, and $K = 10,000$. The results are shown in Fig. 5. Again, there are a few points we can conclude from this experiment:

- 1) Interestingly, for a small size of the training data, K , the empirical MSE of the sLMMSE estimator outperforms the MSE of the sWLMME estimator for almost any value of η . This occurs, as discussed above in Subsection III-B4, due to the fact that the number of unknowns in the sWLMME estimator is larger than that of the sLMMSE estimator, and thus, the sLMMSE estimator provides a more reliable estimate compared to the WLMME estimator for a small size of the training data. This is in contrast with the theoretical MSEs of the WLMME and LMMSE estimators [43]. Thus, this result emphasizes the need for widely-linear estimators, but with fewer parameters to estimate, such as the GSP estimators.
- 2) The MSEs of the GSP estimators (GSP-LMMSE and GSP-WLMME estimators) outperform the MSEs of the conventional estimators (LMMSE and WLMME estimators) for any value of η for $K = 1,000$ and $10,000$, for both the theoretical and the empirical values.
- 3) The MSE of the GSP-WLMME estimator is much smaller than that of the GSP-LMMSE estimator for any value of the non-circularity coefficient, η , for both the theoretical and the empirical values. These MSEs almost coincide for $\eta \approx 0.7$. This result can be explained by the fact that for this value the graph signal becomes proper and circular, and there is no statistical benefit in using

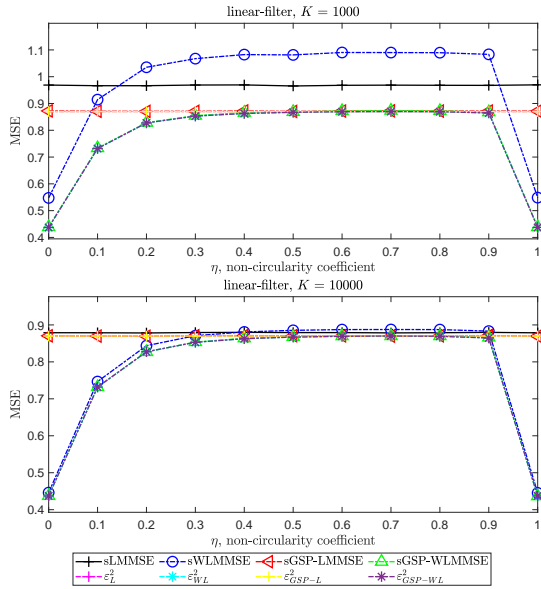


Fig. 5: The theoretical MSEs, ε_L^2 , ε_{WL}^2 , ε_{GSP-L}^2 , and ε_{GSP-WL}^2 , and the empirical MSEs of the sLMMSE, sWLMME, sGSP-LMMSE, and sGSP-WLMMSE estimators for the linear system of Example 1 versus the non-circularity coefficient, η , and for $K = 1,000, 10,000$.

the complementary covariance matrix; thus, both estimators provide identical results, as shown theoretically in Subsection IV-A.

B. Example 2: Synthetic nonlinear system

We further evaluated the performance of the estimators for a nonlinear graph system for the graph used in Example 1 with $N = 100$ nodes. The observed graph signal is given by

$$\mathbf{y} = \text{diag}(\mathbf{x})\mathbf{H}\mathbf{x}^* + \mathbf{n}, \quad (56)$$

where $\mathbf{n} \in \mathbb{R}^N$ is a zero-mean proper Gaussian distributed random graph signal with a covariance matrix $\sigma^2\mathbf{I}_N$ that is independent of \mathbf{x} , and the graph filter is an ARMA filter as defined in (53)-(54). The graph signal \mathbf{x} is now given by

$$\mathbf{x} = (1 + 0.1\boldsymbol{\mu}) \odot e^{j\boldsymbol{\phi}}, \quad (57)$$

where $\boldsymbol{\mu} \in \mathbb{R}^N$ is a vector with i.i.d. entries, in which the n th entry is distributed according to $\mu(n) \sim \mathcal{N}(0, 1)$. In addition, $\boldsymbol{\phi} \in \mathbb{R}^N$ is a vector with i.i.d. entries, in which the n th entry is distributed according to $\phi(n) \sim \mathcal{U}(0, \theta)$, where θ is the upper limit of the phase interval. Clearly, as θ (measured in radians) is closer to 2π , the graph signal \mathbf{x} becomes proper and circular. This kind of signal structure is used as it resembles the common voltage signal in AC power networks, which is later discussed in Subsection V-C. Since the optimal estimators and their MSEs are intractable for this nonlinear filter case, only the empirical MSEs of the sample-mean versions of the estimators are presented in the following results.

The empirical MSEs of the sLMMSE, sWLMME, sGSP-LMMSE, and sGSP-WLMMSE estimators are presented in Fig. 6 for the nonlinear system versus the size of the training data set, K , for the phase maximal values $\theta =$

0.1, 0.2, 0.3, 0.4. There are some conclusions that can be drawn from this experiment:

- 1) As can be seen, both the sWLMME and the sGSP-WLMMSE estimators have a smaller MSE than the MSEs of the sLMMSE and the sGSP-LMMSE estimators, especially for a large amount of training data ($K > 1,000$).
- 2) For a small amount of training data ($K < 1,000$) the MSE of the sWLMME estimator diverges and becomes worse than that of the sGSP-LMMSE estimator.
- 3) For any value of θ and K , the MSE of the sGSP-WLMMSE outperforms the MSEs of all other estimators.
- 4) However, as K increases ($K > 10,000$), the MSE of the sGSP-WLMMSE almost coincides with the MSE of the sWLMME estimator.

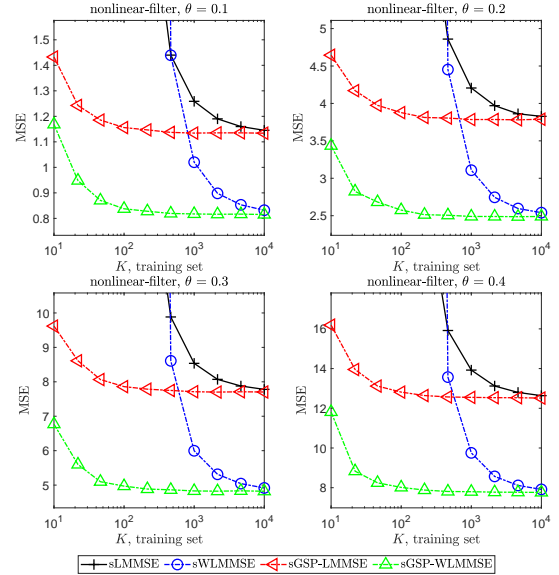


Fig. 6: The empirical MSEs of the sLMMSE, sWLMME, sGSP-LMMSE, and sGSP-WLMMSE estimators for the nonlinear system in Example 2 versus the size of the training data, K , for the maximal phase values $\theta = 0.1, 0.2, 0.3, 0.4$.

C. Example 3: Power System State Estimation (PSSE)

A power system can be represented as an undirected weighted graph, $\mathcal{G}(\mathcal{V}, \xi)$, where the set of vertices, \mathcal{V} , is the set of buses (generators or loads) and the edge set, ξ , is the set of transmission lines between these buses. The system (nodal) admittance matrix is a $N \times N$ complex symmetric matrix, where its (m, k) element is given by (p. 97 in [44])

$$[\mathbf{Y}]_{m,k} = \begin{cases} -\sum_{n \in \mathcal{N}_m} y_{m,n}, & m = k \\ y_{m,k}, & m \neq k \\ 0, & \text{otherwise} \end{cases}, \quad (58)$$

$\forall (m, k) \in \xi$, where $y_{m,k} \in \mathbb{C}$ is the admittance of line (m, k) . The admittance matrix from (58) can be decomposed as follows:

$$\mathbf{Y} = \mathbf{G} + j\mathbf{B}, \quad (59)$$

where the conductance matrix, $\mathbf{G} \in \mathbb{R}^{N \times N}$, and the minus of the susceptance matrix, $-\mathbf{B} \in \mathbb{R}^{N \times N}$, are both real Laplacian

matrices.

The commonly-used nonlinear AC power flow model [44], [45], which is based on Kirchhoff's and Ohm's laws, describes the relation between the complex power injection and voltage phasors. According to this model, the measurement vector of the active and reactive powers can be described by

$$\mathbf{y} = \text{diag}(\mathbf{x})\mathbf{Y}^*\mathbf{x}^* + \mathbf{n}, \quad (60)$$

where $\mathbf{y} \in \mathbb{C}^N$ is the power vector, $\mathbf{x} \in \mathbb{C}^N$ is the voltage vector, and the noise sequence, \mathbf{n} , is a complex circularly symmetric Gaussian i.i.d. random vector with zero mean and a known covariance matrix $\mathbf{R}_n = \sigma^2\mathbf{I}_N$, and is independent of \mathbf{x} . In the graph modeling of the electrical network, the Laplacian matrix, \mathbf{L} , is usually constructed by using $-\mathbf{B}$ (see Subsection II-C in [46]).

The goal of PSSE is to recover the state vector, \mathbf{x} , from the power measurements of \mathbf{y} [47], which is known to be an NP-hard problem. In the following simulations, the values of the different physical parameters in (60) are taken from the test case of a 118-bus IEEE power system [48], where $N = 118$. We assume that the input graph signal, \mathbf{x} , is distributed according to the model expressed in (57). For a given K and a given phase limit, θ , which is implemented according to the model in (60), we generate the sLMMSE, sWLMME, sGSP-LMMSE, and sGSP-WLMME estimators. The empirical MSEs of the sLMMSE, sWLMME, sGSP-LMMSE, and sGSP-WLMME estimators for the PSSE problem are presented in Fig. 7 for $\theta = 0.1, 0.2, 0.3, 0.4$ and different values of K .

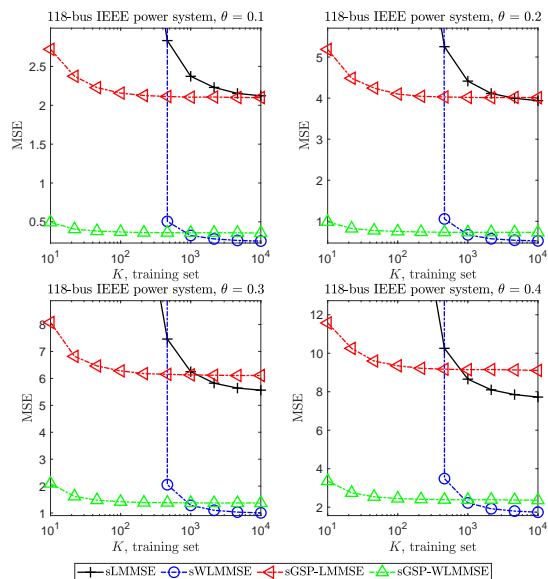


Fig. 7: The empirical MSEs of the sLMMSE, sWLMME, sGSP-LMMSE, and sGSP-WLMME estimators versus K for Example 3 with the 118-bus IEEE power system, for the maximal phase $\theta = 0.1, 0.2, 0.3, 0.4$.

Here are some points we can conclude from this experiment:

- 1) Similar to the nonlinear filter in Example 2, the MSEs of the sWLMME and the sGSP-WLMME estimators are smaller than the MSEs of the sLMMSE and the sGSP-LMMSE estimators, especially for a large amount of training dataset ($K > 750$). Still, for a small K , the MSEs of the sLMMSE and the sWLMME estimators

diverge and become worse than those of the widely-linear (sGSP-LMMSE and sGSP-WLMME) estimators.

- 2) For any value of the phase θ and any K , the MSE of the sGSP-WLMME estimator is lower than the MSEs of the sGSP-LMMSE and the sLMMSE estimators.
- 3) However, the MSE of the sGSP-WLMME estimator is still larger than the MSE of the sWLMME estimator for any value of the maximal phase, θ , and large K .

We also examined the robustness of the estimators to model mismatch due to changes in the topology of the graph. We consider topology changes due to removal or addition of edges in the graph. We assume that the noise standard deviation is $\sigma = 0.01$, and that the number of training dataset is $K = 1,000$. We also assume that the signal phase limit is $\theta = 0.2$. The number of added or removed edges in the graph varies from 1 to 20. For each value of edges, we randomly selected the same number of nodes in the graph and removed (or added) a single edge from (to) their neighborhood. The MSE results are shown in Fig. 8. As can be seen, the sLMMSE estimator has the worst MSE performance in case of edge removal (upper plot of Fig. 8), while the sWLMME estimator has the worst MSE performance in case of edge addition (lower plot of Fig. 8). Both the sGSP-LMMSE and the sGSP-WLMME estimators are robust and the change in their MSE is less affected by the changes in the graph topology compared with the sLMMSE and sWLMME estimators.

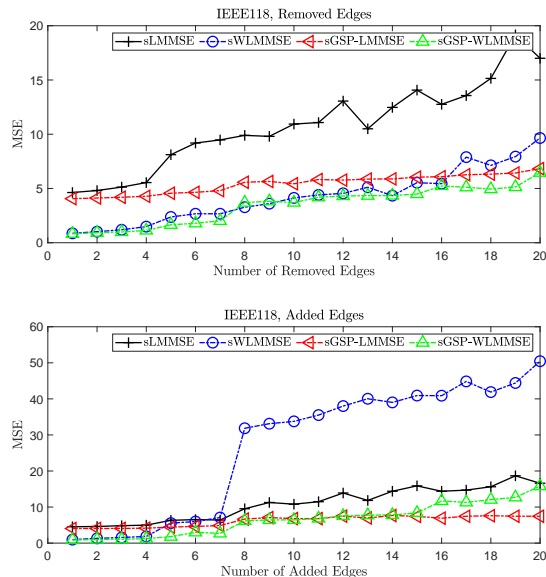


Fig. 8: The empirical MSEs of the sLMMSE, sWLMME, sGSP-LMMSE, and sGSP-WLMME estimators versus the number of added or removed edges in the graph for maximal phase value $\theta = 0.2$, and the size of training dataset in $K = 1,000$.

VI. CONCLUSION

In this paper, we show that taking into consideration widely-linear systems in networks instead of strictly linear ones can yield significant improvements in the estimation of complex-valued graph signals. A straightforward way to perform LMMSE and WLMME filters on graph signals is to apply

them in the graph node domain. However, as such processing may involve a large computation burden and ignores the graph structure behind the data, herein we suggest a reduced-complexity approach where the processing is performed in the graph frequency domain. In particular, we develop the GSP-WLMMSE estimator, which minimizes the MSE among the subset of widely-linear estimators that are represented as an output of two graph filters, where the inputs are the observation vector and its conjugate. It is shown that, in contrast to the proper complex-valued graph signal, the GSP-WLMMSE estimator of improper graph signals also requires the complementary auto-correlation and cross-correlation matrices. We investigate the properties of the GSP-WLMMSE estimator, its behavior under some special cases, and the conditions for the GSP-WLMMSE estimator to coincide with the WLMMSE estimator or with the GSP-LMMSE estimator. If the distributions of the graph signal and the observations are intractable, the sample-mean versions of the different estimators can be used. The diagonal structure of the of the sample-mean estimators, sGSP-LMMSE and sGSP-WLMMSE, in the graph frequency domain bypasses the requirement for an extensive dataset in order to obtain a stable sample-mean estimators, sLMSSE and sWLMMSE, and thus has practical advantages.

In the simulations, we examine synthetic examples and the practical problem of state estimation in power systems. We show that for these problems, the proposed sample-mean version of the GSP-WLMMSE estimator achieves lower MSE than the linear estimators and the WLMMSE estimator for a limited training dataset. For sufficiently large datasets, the sGSP-WLMMSE estimator coincides with the sample-WLMMSE estimator, and they both outperform the linear estimators. Thus, widely-linear GSP estimation can yield significant improvements in the MSE compared to strictly linear graph filters, when the circularity assumption does not hold.

APPENDIX A: PROOF OF THEOREM 1

In this appendix, we develop the GSP-WLMMSE estimator, which is the estimator that minimizes the MSE over the subset of widely-linear GSP estimators in the form of (20). For the sake of simplicity, in this appendix we replace $\mathbf{f}_i(\boldsymbol{\lambda})$ by \mathbf{f}_i , $i = 1, 2$. By substituting (20) in the MSE definition, one obtains

$$\begin{aligned} \mathbb{E}[\|\hat{\mathbf{x}} - \mathbf{x}\|^2] &= \mathbb{E}[\|\mathbf{V}(\text{diag}(\mathbf{f}_1)\bar{\mathbf{y}} + \text{diag}(\mathbf{f}_2)\bar{\mathbf{y}}^* - \mathbf{V}^T \mathbf{x})\|^2] \\ &= \mathbb{E}[\|\text{diag}(\mathbf{f}_1)\bar{\mathbf{y}} + \text{diag}(\mathbf{f}_2)\bar{\mathbf{y}}^* - \bar{\mathbf{x}}\|^2], \end{aligned} \quad (61)$$

where we use the fact that \mathbf{V} is a unitary matrix, i.e. $\mathbf{V}^T \mathbf{V} = \mathbf{V} \mathbf{V}^T = \mathbf{I}$, and that $\bar{\mathbf{x}} = \mathbf{V}^T \mathbf{x}$. Applying the trace operator on (61), and using the trace operator properties, the MSE in (61) can be written as

$$\begin{aligned} \mathbb{E}[\|\hat{\mathbf{x}} - \mathbf{x}\|^2] &= \mathbf{f}_1^H \text{ddiag}(\mathbb{E}[\bar{\mathbf{y}}^* \bar{\mathbf{y}}^T]) \mathbf{f}_1 + \mathbf{f}_2^H \text{ddiag}(\mathbb{E}[\bar{\mathbf{y}} \bar{\mathbf{y}}^H]) \mathbf{f}_2 \\ &\quad + \mathbf{f}_2^H \text{ddiag}(\mathbb{E}[\bar{\mathbf{y}} \bar{\mathbf{y}}^T]) \mathbf{f}_1 + \mathbf{f}_1^H \text{ddiag}(\mathbb{E}[\bar{\mathbf{y}}^* \bar{\mathbf{y}}^H]) \mathbf{f}_2 \\ &\quad - \mathbf{1}^T \text{ddiag}(\mathbb{E}[\bar{\mathbf{x}}^* \bar{\mathbf{y}}^T]) \mathbf{f}_1 - \mathbf{1}^T \text{ddiag}(\mathbb{E}[\bar{\mathbf{x}}^* \bar{\mathbf{y}}^H]) \mathbf{f}_2 \\ &\quad - \mathbf{f}_1^H \text{ddiag}(\mathbb{E}[\bar{\mathbf{y}}^* \bar{\mathbf{x}}^T]) \mathbf{1} - \mathbf{f}_2^H \text{ddiag}(\mathbb{E}[\bar{\mathbf{y}} \bar{\mathbf{x}}^T]) \mathbf{1} \\ &\quad + \mathbb{E}[\bar{\mathbf{x}}^H \bar{\mathbf{x}}] \end{aligned} \quad (62)$$

Since (62) is a convex function of the pair $\mathbf{f}_1, \mathbf{f}_2$, the optimal graph filters are obtained by equating the derivative of the

MSE in (62) w.r.t. $\mathbf{f}_1, \mathbf{f}_2$ to zero (by using complex derivative rules, see e.g. Appendix 2 in [14]), which results in

$$\begin{bmatrix} (\mathbf{D}_{\bar{\mathbf{y}}\bar{\mathbf{y}}}^{\Gamma})^* & (\mathbf{D}_{\bar{\mathbf{y}}\bar{\mathbf{y}}}^{\mathbf{C}})^* \\ \mathbf{D}_{\bar{\mathbf{y}}\bar{\mathbf{y}}}^{\mathbf{C}} & \mathbf{D}_{\bar{\mathbf{y}}\bar{\mathbf{y}}}^{\Gamma} \end{bmatrix} \begin{bmatrix} \hat{\mathbf{f}}_1 \\ \hat{\mathbf{f}}_2 \end{bmatrix} = \begin{bmatrix} (\mathbf{d}_{\bar{\mathbf{y}}\bar{\mathbf{x}}}^{\Gamma})^* \\ \mathbf{d}_{\bar{\mathbf{y}}\bar{\mathbf{x}}}^{\mathbf{C}} \end{bmatrix}, \quad (63)$$

where $\mathbf{d}_{\bar{\mathbf{y}}\bar{\mathbf{x}}}^{\Gamma} \triangleq \text{diag}(\Gamma_{\bar{\mathbf{y}}\bar{\mathbf{x}}})$ and $\mathbf{d}_{\bar{\mathbf{y}}\bar{\mathbf{x}}}^{\mathbf{C}} \triangleq \text{diag}(\mathbf{C}_{\bar{\mathbf{y}}\bar{\mathbf{x}}})$, and $\mathbf{D}_{\bar{\mathbf{y}}\bar{\mathbf{y}}}^{\Gamma}$ and $\mathbf{D}_{\bar{\mathbf{y}}\bar{\mathbf{y}}}^{\mathbf{C}}$ are defined in (18) and (21), respectively. Applying the matrix inversion lemma on (63) leads to

$$\begin{aligned} \hat{\mathbf{f}}_1 &= (\mathbf{D}_{\bar{\mathbf{y}}\bar{\mathbf{y}}}^{\mathbf{P}})^{-1} (\mathbf{d}_{\bar{\mathbf{y}}\bar{\mathbf{x}}}^{\Gamma})^* - (\mathbf{D}_{\bar{\mathbf{y}}\bar{\mathbf{y}}}^{\mathbf{P}})^{-1} (\mathbf{D}_{\bar{\mathbf{y}}\bar{\mathbf{y}}}^{\mathbf{C}})^* (\mathbf{D}_{\bar{\mathbf{y}}\bar{\mathbf{y}}}^{\Gamma})^{-1} \mathbf{d}_{\bar{\mathbf{y}}\bar{\mathbf{x}}}^{\mathbf{C}} \\ &= (\mathbf{D}_{\bar{\mathbf{y}}\bar{\mathbf{y}}}^{\mathbf{P}})^{-1} ((\mathbf{d}_{\bar{\mathbf{y}}\bar{\mathbf{x}}}^{\Gamma})^* - (\mathbf{D}_{\bar{\mathbf{y}}\bar{\mathbf{y}}}^{\mathbf{C}})^* (\mathbf{D}_{\bar{\mathbf{y}}\bar{\mathbf{y}}}^{\Gamma})^{-1} \mathbf{d}_{\bar{\mathbf{y}}\bar{\mathbf{x}}}^{\mathbf{C}}) \end{aligned} \quad (64)$$

and

$$\begin{aligned} \hat{\mathbf{f}}_2 &= -(\mathbf{D}_{\bar{\mathbf{y}}\bar{\mathbf{y}}}^{\mathbf{P}})^{-1} \mathbf{D}_{\bar{\mathbf{y}}\bar{\mathbf{y}}}^{\mathbf{C}} (\mathbf{D}_{\bar{\mathbf{y}}\bar{\mathbf{y}}}^{\Gamma})^{-*} (\mathbf{d}_{\bar{\mathbf{y}}\bar{\mathbf{x}}}^{\Gamma})^* + (\mathbf{D}_{\bar{\mathbf{y}}\bar{\mathbf{y}}}^{\mathbf{P}})^{-1} \mathbf{d}_{\bar{\mathbf{y}}\bar{\mathbf{x}}}^{\mathbf{C}} \\ &= (\mathbf{D}_{\bar{\mathbf{y}}\bar{\mathbf{y}}}^{\mathbf{P}})^{-1} (\mathbf{d}_{\bar{\mathbf{y}}\bar{\mathbf{x}}}^{\mathbf{C}} - \mathbf{D}_{\bar{\mathbf{y}}\bar{\mathbf{y}}}^{\mathbf{C}} (\mathbf{D}_{\bar{\mathbf{y}}\bar{\mathbf{y}}}^{\Gamma})^{-1} (\mathbf{d}_{\bar{\mathbf{y}}\bar{\mathbf{x}}}^{\Gamma})^*), \end{aligned} \quad (65)$$

where $\mathbf{D}_{\bar{\mathbf{y}}\bar{\mathbf{y}}}^{\Gamma}$ is a real matrix, and the Schur complement of the left matrix in (63), $\mathbf{D}_{\bar{\mathbf{y}}\bar{\mathbf{y}}}^{\mathbf{P}}$, is defined in (26) and is a real diagonal matrix (thus, we used $(\mathbf{D}_{\bar{\mathbf{y}}\bar{\mathbf{y}}}^{\mathbf{P}})^* = \mathbf{D}_{\bar{\mathbf{y}}\bar{\mathbf{y}}}^{\mathbf{P}}$ and $(\mathbf{D}_{\bar{\mathbf{y}}\bar{\mathbf{y}}}^{\mathbf{P}})^{-H} = (\mathbf{D}_{\bar{\mathbf{y}}\bar{\mathbf{y}}}^{\mathbf{P}})^{-1}$). Equivalently, the n th elements of $\hat{\mathbf{f}}_2$ and $\hat{\mathbf{f}}_1$ satisfy

$$\hat{f}_{1,n} = \frac{([\Gamma_{\bar{\mathbf{y}}\bar{\mathbf{x}}}]_{n,n})^* ([\Gamma_{\bar{\mathbf{y}}\bar{\mathbf{y}}}]_{n,n}) - [\mathbf{C}_{\bar{\mathbf{y}}\bar{\mathbf{x}}}]_{n,n} ([\mathbf{C}_{\bar{\mathbf{y}}\bar{\mathbf{y}}}]_{n,n})^*}{|[\Gamma_{\bar{\mathbf{y}}\bar{\mathbf{y}}}]_{n,n}|^2 - |[\mathbf{C}_{\bar{\mathbf{y}}\bar{\mathbf{y}}}]_{n,n}|^2}, \quad (66)$$

$$\hat{f}_{2,n} = \frac{[\mathbf{C}_{\bar{\mathbf{y}}\bar{\mathbf{x}}}]_{n,n} [\Gamma_{\bar{\mathbf{y}}\bar{\mathbf{y}}}]_{n,n} - ([\Gamma_{\bar{\mathbf{y}}\bar{\mathbf{x}}}]_{n,n})^* [\mathbf{C}_{\bar{\mathbf{y}}\bar{\mathbf{y}}}]_{n,n}}{|[\Gamma_{\bar{\mathbf{y}}\bar{\mathbf{y}}}]_{n,n}|^2 - |[\mathbf{C}_{\bar{\mathbf{y}}\bar{\mathbf{y}}}]_{n,n}|^2}, \quad (67)$$

for any $n = 1, \dots, N$. Now, if $\rho_n \neq 1$, where ρ_n is defined in (22), then (66) and (67) can be written as

$$\hat{f}_{1,n} = \frac{1}{1 - \rho_n} \frac{([\Gamma_{\bar{\mathbf{y}}\bar{\mathbf{x}}}]_{n,n})^*}{[\Gamma_{\bar{\mathbf{y}}\bar{\mathbf{y}}}]_{n,n}} + \left(1 - \frac{1}{1 - \rho_n}\right) \frac{[\mathbf{C}_{\bar{\mathbf{y}}\bar{\mathbf{x}}}]_{n,n}}{[\mathbf{C}_{\bar{\mathbf{y}}\bar{\mathbf{y}}}]_{n,n}} \quad (68)$$

$$\hat{f}_{2,n} = \frac{1}{1 - \rho_n} \frac{[\mathbf{C}_{\bar{\mathbf{y}}\bar{\mathbf{x}}}]_{n,n}}{([\Gamma_{\bar{\mathbf{y}}\bar{\mathbf{y}}}]_{n,n})^*} + \left(1 - \frac{1}{1 - \rho_n}\right) \frac{([\Gamma_{\bar{\mathbf{y}}\bar{\mathbf{x}}}]_{n,n})^*}{([\mathbf{C}_{\bar{\mathbf{y}}\bar{\mathbf{y}}}]_{n,n})^*}. \quad (69)$$

By substituting (68) and (69) in (20), we obtain the GSP-WLMMSE estimator in (23).

APPENDIX B: DEVELOPMENT OF THE ORTHOGONALITY PRINCIPLE

In this appendix we develop the orthogonality principle of the GSP-WLMMSE estimator. Using (25), we obtain

$$\begin{aligned} \mathbb{E}[(\hat{\mathbf{x}}^{(\text{GSP-WLMMSE})} - \mathbf{x})^H \mathbf{y}] &= -\mathbb{E}[\mathbf{x}^H \mathbf{y}] \\ &\quad + \mathbb{E}[\bar{\mathbf{y}}^H (\mathbf{D}_{\bar{\mathbf{y}}\bar{\mathbf{y}}}^{\mathbf{P}})^{-1} (\mathbf{D}_{\bar{\mathbf{x}}\bar{\mathbf{y}}}^{\Gamma} - (\mathbf{D}_{\bar{\mathbf{y}}\bar{\mathbf{y}}}^{\mathbf{C}})^* (\mathbf{D}_{\bar{\mathbf{y}}\bar{\mathbf{y}}}^{\Gamma})^{-1} \mathbf{D}_{\bar{\mathbf{y}}\bar{\mathbf{x}}}^{\mathbf{C}})^H \bar{\mathbf{y}}] \\ &\quad + \mathbb{E}[\bar{\mathbf{y}}^T (\mathbf{D}_{\bar{\mathbf{y}}\bar{\mathbf{y}}}^{\mathbf{P}})^{-1} ((\mathbf{D}_{\bar{\mathbf{y}}\bar{\mathbf{x}}}^{\mathbf{C}} - \mathbf{D}_{\bar{\mathbf{y}}\bar{\mathbf{y}}}^{\mathbf{C}} (\mathbf{D}_{\bar{\mathbf{y}}\bar{\mathbf{y}}}^{\Gamma})^{-1} (\mathbf{D}_{\bar{\mathbf{y}}\bar{\mathbf{x}}}^{\Gamma})^*)^H \bar{\mathbf{y}}], \end{aligned} \quad (70)$$

where we used (15) and the fact that \mathbf{V} and $\mathbf{D}_{\bar{\mathbf{y}}\bar{\mathbf{y}}}^{\Gamma}$ are real matrices. By using the trace operator properties and the fact that $\mathbb{E}[\mathbf{x}^H \mathbf{y}] = \mathbb{E}[\mathbf{x}^H \mathbf{V} \mathbf{V}^T \mathbf{y}] = \text{tr}(\Gamma_{\bar{\mathbf{y}}\bar{\mathbf{x}}})$, we obtain that (70) can be rewritten as

$$\begin{aligned} \mathbb{E}[(\hat{\mathbf{x}}^{(\text{GSP-WLMMSE})} - \mathbf{x})^H \mathbf{y}] &= -\text{tr}(\Gamma_{\bar{\mathbf{y}}\bar{\mathbf{x}}}) \\ &\quad \text{tr}((\mathbf{D}_{\bar{\mathbf{y}}\bar{\mathbf{y}}}^{\mathbf{P}})^{-1} (\mathbf{D}_{\bar{\mathbf{x}}\bar{\mathbf{y}}}^{\Gamma} - (\mathbf{D}_{\bar{\mathbf{y}}\bar{\mathbf{y}}}^{\mathbf{C}})^* (\mathbf{D}_{\bar{\mathbf{y}}\bar{\mathbf{y}}}^{\Gamma})^{-1} \mathbf{D}_{\bar{\mathbf{y}}\bar{\mathbf{x}}}^{\mathbf{C}})^H \Gamma_{\bar{\mathbf{y}}\bar{\mathbf{y}}}) \\ &\quad + \text{tr}((\mathbf{D}_{\bar{\mathbf{y}}\bar{\mathbf{y}}}^{\mathbf{P}})^{-1} ((\mathbf{D}_{\bar{\mathbf{y}}\bar{\mathbf{x}}}^{\mathbf{C}} - \mathbf{D}_{\bar{\mathbf{y}}\bar{\mathbf{y}}}^{\mathbf{C}} (\mathbf{D}_{\bar{\mathbf{y}}\bar{\mathbf{y}}}^{\Gamma})^{-*} (\mathbf{D}_{\bar{\mathbf{y}}\bar{\mathbf{x}}}^{\Gamma})^*)^H \mathbf{C}_{\bar{\mathbf{y}}\bar{\mathbf{y}}}) \\ &\quad = -\text{tr}(\mathbf{D}_{\bar{\mathbf{y}}\bar{\mathbf{x}}}^{\Gamma}) \\ &\quad \text{tr}((\mathbf{D}_{\bar{\mathbf{y}}\bar{\mathbf{y}}}^{\mathbf{P}})^{-1} (\mathbf{D}_{\bar{\mathbf{x}}\bar{\mathbf{y}}}^{\Gamma} - (\mathbf{D}_{\bar{\mathbf{y}}\bar{\mathbf{y}}}^{\mathbf{C}})^* (\mathbf{D}_{\bar{\mathbf{y}}\bar{\mathbf{y}}}^{\Gamma})^{-1} \mathbf{D}_{\bar{\mathbf{y}}\bar{\mathbf{x}}}^{\mathbf{C}})^H \mathbf{D}_{\bar{\mathbf{y}}\bar{\mathbf{y}}}^{\Gamma}) \\ &\quad + \text{tr}((\mathbf{D}_{\bar{\mathbf{y}}\bar{\mathbf{y}}}^{\mathbf{P}})^{-1} ((\mathbf{D}_{\bar{\mathbf{y}}\bar{\mathbf{x}}}^{\mathbf{C}} - \mathbf{D}_{\bar{\mathbf{y}}\bar{\mathbf{y}}}^{\mathbf{C}} (\mathbf{D}_{\bar{\mathbf{y}}\bar{\mathbf{y}}}^{\Gamma})^{-*} (\mathbf{D}_{\bar{\mathbf{y}}\bar{\mathbf{x}}}^{\Gamma})^*)^H \mathbf{D}_{\bar{\mathbf{y}}\bar{\mathbf{y}}}^{\mathbf{C}}), \end{aligned} \quad (71)$$

where the last equality is obtained by using the definitions in (18) and (21), and since $\text{tr}(\mathbf{D}\mathbf{A}) = \text{tr}(\mathbf{D}\text{ddiag}(\mathbf{A}))$ for any diagonal matrix \mathbf{D} . By substituting (26) in (71), it can be verified that $\mathbb{E}[(\hat{\mathbf{x}}^{(\text{GSP-WLMMSE})} - \mathbf{x})^H \mathbf{y}] = 0$. Similarly, it can be shown that $\mathbb{E}[(\hat{\mathbf{x}}^{(\text{GSP-WLMMSE})} - \mathbf{x})^H \mathbf{y}^*] = 0$.

APPENDIX C: PROOF OF THEOREM 2

In this appendix, we develop the explicit terms of the trace of the MSE of the GSP-LMMSE estimator from (17) and of the GSP-WLMMSE estimator from (23). The proof is along the lines of the proof of [43, Eq. (1.39)] for the WLMSE estimator. For the sake of simplicity, in this appendix we replace $\mathbf{f}_i(\boldsymbol{\lambda})$ by $\hat{\mathbf{f}}_i$ for $i = 1, 2$.

According to the orthogonality principle of the GSP-WLMMSE estimator, developed in Appendix B, $\mathbb{E}[(\hat{\mathbf{x}}^{(\text{GSP-WLMMSE})} - \mathbf{x})^H \mathbf{y}] = 0$ and $\mathbb{E}[(\hat{\mathbf{x}}^{(\text{GSP-WLMMSE})} - \mathbf{x})^H \mathbf{y}^*] = 0$. In other words, the error vector of the GSP-WLMMSE estimator is orthogonal to any linear combination of these vectors. Since the estimate $\hat{\mathbf{x}}^{(\text{GSP-WLMMSE})}$ is a linear combination of \mathbf{y} and \mathbf{y}^* then, $(\hat{\mathbf{x}}^{(\text{GSP-WLMMSE})} - \mathbf{x}) \perp \hat{\mathbf{x}}^{(\text{GSP-WLMMSE})}$, and as a result, we obtain that

$$\mathbb{E}[\|\hat{\mathbf{x}}^{(\text{GSP-WLMMSE})}\|^2] = \mathbb{E}[(\hat{\mathbf{x}}^{(\text{GSP-WLMMSE})})^H \mathbf{x}]. \quad (72)$$

Thus, the trace of the MSE of the GSP-WLMMSE estimator is given by

$$\begin{aligned} \varepsilon_{\text{GSP-WL}}^2 &= \mathbb{E}[\|\hat{\mathbf{x}}^{(\text{GSP-WLMMSE})} - \mathbf{x}\|^2] \\ &= \mathbb{E}[\|\mathbf{x}\|^2] - \mathbb{E}[\|\hat{\mathbf{x}}^{(\text{GSP-WLMMSE})}\|^2]. \end{aligned} \quad (73)$$

By substituting the estimator $\hat{\mathbf{x}}^{(\text{GSP-WLMMSE})}$, which is a widely-linear GSP estimator described by (20) with the optimal graph frequency responses $\hat{\mathbf{f}}_1$ and $\hat{\mathbf{f}}_2$ from Appendix A, and after a few algebraic steps, the MSE in (73) is also expressed in a compact form as

$$\begin{aligned} \varepsilon_{\text{GSP-WL}}^2 &= \text{tr}(\boldsymbol{\Gamma}_{\mathbf{xx}}) \\ &\quad - \begin{bmatrix} \hat{\mathbf{f}}_1 \\ \hat{\mathbf{f}}_2 \end{bmatrix}^H \begin{bmatrix} (\mathbf{D}_{\hat{\mathbf{y}\hat{\mathbf{y}}}}^{\Gamma})^* & (\mathbf{D}_{\hat{\mathbf{y}\hat{\mathbf{y}}}}^{\mathbf{C}})^* \\ \mathbf{D}_{\hat{\mathbf{y}\hat{\mathbf{y}}} }^{\mathbf{C}} & \mathbf{D}_{\hat{\mathbf{y}\hat{\mathbf{y}}} }^{\Gamma} \end{bmatrix} \begin{bmatrix} \hat{\mathbf{f}}_1 \\ \hat{\mathbf{f}}_2 \end{bmatrix} \\ &= \text{tr}(\boldsymbol{\Gamma}_{\mathbf{xx}}) - \begin{bmatrix} (\mathbf{d}_{\hat{\mathbf{y}\hat{\mathbf{x}}} }^{\Gamma})^* \\ \mathbf{d}_{\hat{\mathbf{y}\hat{\mathbf{x}}} }^{\mathbf{C}} \end{bmatrix}^H \\ &\quad \times \begin{bmatrix} \mathbf{D}_{\hat{\mathbf{y}\hat{\mathbf{y}}} }^{\Gamma} & (\mathbf{D}_{\hat{\mathbf{y}\hat{\mathbf{y}}} }^{\mathbf{C}})^* \\ \mathbf{D}_{\hat{\mathbf{y}\hat{\mathbf{y}}} }^{\mathbf{C}} & \mathbf{D}_{\hat{\mathbf{y}\hat{\mathbf{y}}} }^{\Gamma} \end{bmatrix}^{-1} \begin{bmatrix} (\mathbf{d}_{\hat{\mathbf{y}\hat{\mathbf{x}}} }^{\Gamma})^* \\ \mathbf{d}_{\hat{\mathbf{y}\hat{\mathbf{x}}} }^{\mathbf{C}} \end{bmatrix}, \end{aligned} \quad (74)$$

where the last equality is obtained by substituting (63) and using $(\mathbf{D}_{\hat{\mathbf{y}\hat{\mathbf{y}}} }^{\Gamma})^* = \mathbf{D}_{\hat{\mathbf{y}\hat{\mathbf{y}}} }^{\Gamma}$. By using the inverse of a block matrix, (74) can be rewritten as

$$\begin{aligned} \varepsilon_{\text{GSP-WL}}^2 &= \text{tr}(\boldsymbol{\Gamma}_{\mathbf{xx}}) - \begin{bmatrix} (\mathbf{d}_{\hat{\mathbf{y}\hat{\mathbf{x}}} }^{\Gamma})^* \\ \mathbf{d}_{\hat{\mathbf{y}\hat{\mathbf{x}}} }^{\mathbf{C}} \end{bmatrix}^H \\ &\quad \times \begin{bmatrix} (\mathbf{D}_{\hat{\mathbf{y}\hat{\mathbf{y}}} }^{\mathbf{P}})^{-1} & \mathbf{E}_{1,2} \\ \mathbf{E}_{2,1} & (\mathbf{D}_{\hat{\mathbf{y}\hat{\mathbf{y}}} }^{\mathbf{P}})^{-1} \end{bmatrix} \begin{bmatrix} (\mathbf{d}_{\hat{\mathbf{y}\hat{\mathbf{x}}} }^{\Gamma})^* \\ \mathbf{d}_{\hat{\mathbf{y}\hat{\mathbf{x}}} }^{\mathbf{C}} \end{bmatrix}, \end{aligned} \quad (75)$$

where the off-diagonal blocks are

$$\mathbf{E}_{12} = -(\mathbf{D}_{\hat{\mathbf{y}\hat{\mathbf{y}}} }^{\mathbf{P}})^{-1} (\mathbf{D}_{\hat{\mathbf{y}\hat{\mathbf{y}}} }^{\mathbf{C}})^* (\mathbf{D}_{\hat{\mathbf{y}\hat{\mathbf{y}}} }^{\Gamma})^{-1} \quad (76)$$

$$\mathbf{E}_{21} = -(\mathbf{D}_{\hat{\mathbf{y}\hat{\mathbf{y}}} }^{\mathbf{P}})^{-1} \mathbf{D}_{\hat{\mathbf{y}\hat{\mathbf{y}}} }^{\mathbf{C}} (\mathbf{D}_{\hat{\mathbf{y}\hat{\mathbf{y}}} }^{\Gamma})^{-1}, \quad (77)$$

and the Schur complement $\mathbf{D}_{\hat{\mathbf{y}\hat{\mathbf{y}}} }^{\mathbf{P}}$ is defined in (26) and is a real diagonal matrix.

On the other hand, by using (17), it can be shown that the trace of the MSE of the GSP-LMMSE estimator is

$$\begin{aligned} \varepsilon_{\text{GSP-L}}^2 &= \mathbb{E}[\|\hat{\mathbf{x}}^{(\text{GSP-LMMSE})} - \mathbf{x}\|^2] \\ &= \text{tr}(\boldsymbol{\Gamma}_{\mathbf{xx}}) - (\mathbf{d}_{\hat{\mathbf{y}\hat{\mathbf{x}}} }^{\Gamma})^T (\mathbf{D}_{\hat{\mathbf{y}\hat{\mathbf{y}}} }^{\Gamma})^{-*} (\mathbf{d}_{\hat{\mathbf{y}\hat{\mathbf{x}}} }^{\Gamma})^*, \end{aligned} \quad (78)$$

which can also be expressed in an equivalent way as

$$\begin{aligned} \varepsilon_{\text{GSP-L}}^2 &= \text{tr}(\boldsymbol{\Gamma}_{\mathbf{xx}}) \\ &\quad - \begin{bmatrix} (\mathbf{d}_{\hat{\mathbf{y}\hat{\mathbf{x}}} }^{\Gamma})^* \\ \mathbf{d}_{\hat{\mathbf{y}\hat{\mathbf{x}}} }^{\mathbf{C}} \end{bmatrix}^H \begin{bmatrix} (\mathbf{D}_{\hat{\mathbf{y}\hat{\mathbf{y}}} }^{\Gamma})^{-*} & \mathbf{0} \\ \mathbf{0} & \mathbf{0} \end{bmatrix} \begin{bmatrix} (\mathbf{d}_{\hat{\mathbf{y}\hat{\mathbf{x}}} }^{\Gamma})^* \\ \mathbf{d}_{\hat{\mathbf{y}\hat{\mathbf{x}}} }^{\mathbf{C}} \end{bmatrix}. \end{aligned} \quad (79)$$

The difference between the trace MSEs from (74) and (79) is

$$\begin{aligned} \varepsilon_{\text{GSP-L}}^2 - \varepsilon_{\text{GSP-WL}}^2 &= \begin{bmatrix} (\mathbf{d}_{\hat{\mathbf{y}\hat{\mathbf{x}}} }^{\Gamma})^* \\ \mathbf{d}_{\hat{\mathbf{y}\hat{\mathbf{x}}} }^{\mathbf{C}} \end{bmatrix}^H \\ &\quad \times \begin{bmatrix} (\mathbf{D}_{\hat{\mathbf{y}\hat{\mathbf{y}}} }^{\mathbf{P}})^{-1} - (\mathbf{D}_{\hat{\mathbf{y}\hat{\mathbf{y}}} }^{\Gamma})^{-1} & \mathbf{E}_{1,2} \\ \mathbf{E}_{2,1} & (\mathbf{D}_{\hat{\mathbf{y}\hat{\mathbf{y}}} }^{\mathbf{P}})^{-1} \end{bmatrix} \begin{bmatrix} (\mathbf{d}_{\hat{\mathbf{y}\hat{\mathbf{x}}} }^{\Gamma})^* \\ \mathbf{d}_{\hat{\mathbf{y}\hat{\mathbf{x}}} }^{\mathbf{C}} \end{bmatrix}. \end{aligned} \quad (80)$$

By using (27), it can be verified that

$$\begin{aligned} &(\mathbf{D}_{\hat{\mathbf{y}\hat{\mathbf{y}}} }^{\mathbf{P}})^{-1} - (\mathbf{D}_{\hat{\mathbf{y}\hat{\mathbf{y}}} }^{\Gamma})^{-1} \\ &= (\mathbf{D}_{\hat{\mathbf{y}\hat{\mathbf{y}}} }^{\Gamma})^{-1} (\mathbf{D}_{\hat{\mathbf{y}\hat{\mathbf{y}}} }^{\mathbf{C}})^* (\mathbf{D}_{\hat{\mathbf{y}\hat{\mathbf{y}}} }^{\mathbf{P}})^{-1} \mathbf{D}_{\hat{\mathbf{y}\hat{\mathbf{y}}} }^{\mathbf{C}} (\mathbf{D}_{\hat{\mathbf{y}\hat{\mathbf{y}}} }^{\Gamma})^{-1} \\ &= \mathbf{E}_{2,1} \mathbf{D}_{\hat{\mathbf{y}\hat{\mathbf{y}}} }^{\mathbf{P}} \mathbf{E}_{1,2}, \end{aligned} \quad (81)$$

where we used the fact that $\mathbf{E}_{2,1}, \mathbf{D}_{\hat{\mathbf{y}\hat{\mathbf{y}}} }^{\mathbf{P}}, \mathbf{E}_{1,2}$ are based on multiplications of diagonal matrices, and thus are invariant to changing the order of the multiplications. By substituting (81) in (80) and using the fact that $\mathbf{E}_{2,1} = \mathbf{E}_{1,2}^*$, we obtain that

$$\begin{aligned} \varepsilon_{\text{GSP-L}}^2 - \varepsilon_{\text{GSP-WL}}^2 &= (\mathbf{d}_{\hat{\mathbf{y}\hat{\mathbf{x}}} }^{\Gamma})^T \mathbf{E}_{2,1} \mathbf{D}_{\hat{\mathbf{y}\hat{\mathbf{y}}} }^{\mathbf{P}} \mathbf{E}_{1,2} (\mathbf{d}_{\hat{\mathbf{y}\hat{\mathbf{x}}} }^{\Gamma})^* + (\mathbf{d}_{\hat{\mathbf{y}\hat{\mathbf{x}}} }^{\Gamma})^T \mathbf{E}_{1,2} \mathbf{d}_{\hat{\mathbf{y}\hat{\mathbf{x}}} }^{\mathbf{C}} \\ &\quad + (\mathbf{d}_{\hat{\mathbf{y}\hat{\mathbf{x}}} }^{\mathbf{C}})^H \mathbf{E}_{2,1} (\mathbf{d}_{\hat{\mathbf{y}\hat{\mathbf{x}}} }^{\Gamma})^* + (\mathbf{d}_{\hat{\mathbf{y}\hat{\mathbf{x}}} }^{\mathbf{C}})^H (\mathbf{D}_{\hat{\mathbf{y}\hat{\mathbf{y}}} }^{\mathbf{P}})^{-1} \mathbf{d}_{\hat{\mathbf{y}\hat{\mathbf{x}}} }^{\mathbf{C}} \\ &= (\mathbf{d}_{\hat{\mathbf{y}\hat{\mathbf{x}}} }^{\mathbf{C}} - (\mathbf{D}_{\hat{\mathbf{y}\hat{\mathbf{y}}} }^{\mathbf{C}})^* (\mathbf{D}_{\hat{\mathbf{y}\hat{\mathbf{y}}} }^{\Gamma})^{-1} (\mathbf{d}_{\hat{\mathbf{y}\hat{\mathbf{x}}} }^{\Gamma})^*)^H (\mathbf{D}_{\hat{\mathbf{y}\hat{\mathbf{y}}} }^{\mathbf{P}})^{-1} \\ &\quad \times (\mathbf{d}_{\hat{\mathbf{y}\hat{\mathbf{x}}} }^{\mathbf{C}} - (\mathbf{D}_{\hat{\mathbf{y}\hat{\mathbf{y}}} }^{\mathbf{C}})^* (\mathbf{D}_{\hat{\mathbf{y}\hat{\mathbf{y}}} }^{\Gamma})^{-1} (\mathbf{d}_{\hat{\mathbf{y}\hat{\mathbf{x}}} }^{\Gamma})^*), \end{aligned} \quad (82)$$

where the last equality is obtained by substituting (76) and (77). Finally, by substituting (29) in (82), $\varepsilon_{\text{GSP-L}}^2 - \varepsilon_{\text{GSP-WL}}^2$ can be expressed in a compact form as (30). In particular, it can be seen that the difference between the trace of the MSE of the GSP-LMMSE estimator is always larger than or equal to the trace of the MSE of the GSP-WLMMSE estimator.

APPENDIX D: PROOF OF THEOREM 4

By using (41), we obtain that

$$\begin{aligned} \boldsymbol{\Gamma}_{\hat{\mathbf{y}\hat{\mathbf{y}}}} &= \mathbb{E}[\hat{\mathbf{y}}\hat{\mathbf{y}}^H] = h_1(\boldsymbol{\Lambda}) \boldsymbol{\Gamma}_{\hat{\mathbf{x}\hat{\mathbf{x}}} } h_1^*(\boldsymbol{\Lambda}) + h_2(\boldsymbol{\Lambda}) \boldsymbol{\Gamma}_{\hat{\mathbf{x}\hat{\mathbf{x}}} }^* h_2^*(\boldsymbol{\Lambda}) \\ &\quad + h_1(\boldsymbol{\Lambda}) \mathbf{C}_{\hat{\mathbf{x}\hat{\mathbf{x}}} } h_2^*(\boldsymbol{\Lambda}) + h_2(\boldsymbol{\Lambda}) \mathbf{C}_{\hat{\mathbf{x}\hat{\mathbf{x}}} }^* h_1^*(\boldsymbol{\Lambda}) + \boldsymbol{\Gamma}_{\hat{\mathbf{w}\hat{\mathbf{w}}}}, \end{aligned} \quad (83)$$

where we use the GFT definition in (15). Since according to the Theorem conditions, $\boldsymbol{\Gamma}_{\hat{\mathbf{w}\hat{\mathbf{w}}}}, \boldsymbol{\Gamma}_{\hat{\mathbf{x}\hat{\mathbf{x}}}},$ and $\mathbf{C}_{\hat{\mathbf{x}\hat{\mathbf{x}}}}$ are diagonal matrices, we obtain that $\boldsymbol{\Gamma}_{\hat{\mathbf{y}\hat{\mathbf{y}}}}$ is a diagonal matrix, i.e.

$$\boldsymbol{\Gamma}_{\hat{\mathbf{y}\hat{\mathbf{y}}}} = \mathbf{D}_{\hat{\mathbf{y}\hat{\mathbf{y}}}}^{\Gamma}. \quad (84)$$

Similarly, the following covariance matrices:

$$\begin{aligned} \mathbf{C}_{\hat{\mathbf{y}\hat{\mathbf{y}}}} &= \mathbb{E}[\hat{\mathbf{y}}\hat{\mathbf{y}}^T] = h_1(\boldsymbol{\Lambda}) \mathbf{C}_{\hat{\mathbf{x}\hat{\mathbf{x}}} } h_1(\boldsymbol{\Lambda}) + h_2(\boldsymbol{\Lambda}) \mathbf{C}_{\hat{\mathbf{x}\hat{\mathbf{x}}} }^* h_2(\boldsymbol{\Lambda}) \\ &\quad + h_1(\boldsymbol{\Lambda}) \boldsymbol{\Gamma}_{\hat{\mathbf{x}\hat{\mathbf{x}}} } h_2(\boldsymbol{\Lambda}) + h_2(\boldsymbol{\Lambda}) \boldsymbol{\Gamma}_{\hat{\mathbf{x}\hat{\mathbf{x}}} }^* h_1(\boldsymbol{\Lambda}) + \mathbf{C}_{\hat{\mathbf{w}\hat{\mathbf{w}}}}, \end{aligned} \quad (85)$$

$$\boldsymbol{\Gamma}_{\hat{\mathbf{x}\hat{\mathbf{y}}}} = \mathbb{E}[\hat{\mathbf{x}}\hat{\mathbf{y}}^H] = \boldsymbol{\Gamma}_{\hat{\mathbf{x}\hat{\mathbf{x}}} } h_1^*(\boldsymbol{\Lambda}) + \mathbf{C}_{\hat{\mathbf{x}\hat{\mathbf{x}}} } h_2^*(\boldsymbol{\Lambda}), \quad (86)$$

and

$$\mathbf{C}_{\hat{\mathbf{x}\hat{\mathbf{y}}}} = \mathbb{E}[\hat{\mathbf{x}}\hat{\mathbf{y}}^T] = \mathbf{C}_{\hat{\mathbf{x}\hat{\mathbf{x}}} } h_1(\boldsymbol{\Lambda}) + \boldsymbol{\Gamma}_{\hat{\mathbf{x}\hat{\mathbf{x}}} } h_2(\boldsymbol{\Lambda}), \quad (87)$$

are all diagonal matrices. As a result, the Schur complement from (7) satisfies

$$\mathbf{P}_{yy} = \text{ddiag}(\mathbf{\Gamma}_{yy}) - \text{ddiag}(\mathbf{C}_{yy}) \text{ddiag}((\mathbf{\Gamma}_{yy}^{-1})^*) \text{ddiag}((\mathbf{C}_{yy})^*) = \mathbf{D}_{\bar{y}\bar{y}}^{\mathbf{P}}, \quad (88)$$

where $\mathbf{D}_{\bar{y}\bar{y}}^{\mathbf{P}}$ is defined in (26) and is a real matrix. Therefore, since all the matrices involved are diagonal matrices, (37) and (38) hold.

REFERENCES

- [1] A. Ortega, P. Frossard, J. Kovačević, J. M. F. Moura, and P. Vandergheynst, "Graph signal processing: Overview, challenges, and applications," *Proc. IEEE*, vol. 106, no. 5, pp. 808–828, May 2018.
- [2] D. I. Shuman, S. K. Narang, P. Frossard, A. Ortega, and P. Vandergheynst, "The emerging field of signal processing on graphs: Extending high-dimensional data analysis to networks and other irregular domains," *IEEE Signal Processing Magazine*, vol. 30, no. 3, pp. 83–98, May 2013.
- [3] Y. Tanaka, Y. C. Eldar, A. Ortega, and G. Cheung, "Sampling signals on graphs: From theory to applications," *IEEE Signal Processing Magazine*, vol. 37, no. 6, pp. 14–30, 2020.
- [4] A. Anis, A. Gadde, and A. Ortega, "Towards a sampling theorem for signals on arbitrary graphs," in *Proc. of ICASSP*, May 2014, pp. 3864–3868.
- [5] T. Routtenberg, "Non-Bayesian estimation framework for signal recovery on graphs," *IEEE Trans. Signal Process.*, vol. 69, pp. 1169–1184, 2021.
- [6] A. Kroizer, T. Routtenberg, and Y. C. Eldar, "Bayesian estimation of graph signals," *IEEE Trans. Signal Process.*, vol. 70, pp. 2207–2223, 2022.
- [7] Z. Han, L. Wang, Z. Lin, and R. Zheng, "Formation control with size scaling via a complex Laplacian-based approach," *IEEE Trans. cybernetics*, vol. 46, no. 10, pp. 2348–2359, 2015.
- [8] K. Tscherkaschin, B. Knoop, J. Rust, and S. Paul, "Design of a multi-core hardware architecture for consensus-based MIMO detection algorithms," in *Asilomar Conference on Signals, Systems and Computers*, 2016, pp. 877–881.
- [9] R. Ramakrishna and A. Scaglione, "Grid-graph signal processing (grid-GSP): A graph signal processing framework for the power grid," *IEEE Trans. Signal Process.*, vol. 69, pp. 2725–2739, 2021.
- [10] E. Drayer and T. Routtenberg, "Detection of false data injection attacks in smart grids based on graph signal processing," *IEEE Systems Journal*, vol. 14, no. 2, pp. 1886–1896, 2020.
- [11] L. Dabush, A. Kroizer, and T. Routtenberg, "State estimation in unobservable power systems via graph signal processing tools," 2021. [Online]. Available: <https://arxiv.org/abs/2106.02254>
- [12] J. K. Tugnait, "Graphical lasso for high-dimensional complex gaussian graphical model selection," in *ICASSP 2019 - 2019 IEEE International Conference on Acoustics, Speech and Signal Processing (ICASSP)*, 2019, pp. 2952–2956.
- [13] F. D. Neeser and J. L. Massey, "Proper complex random processes with applications to information theory," *IEEE Trans. information theory*, vol. 39, no. 4, pp. 1293–1302, 1993.
- [14] P. J. Schreier and L. L. Scharf, *Statistical signal processing of complex-valued data: the theory of improper and noncircular signals*. Cambridge university press, 2010.
- [15] T. Nitta, M. Kobayashi, and D. P. Mandic, "Hypercomplex widely linear estimation through the lens of underpinning geometry," *IEEE Trans. Signal Process.*, vol. 67, no. 15, pp. 3985–3994, 2019.
- [16] Y. Xia, S. C. Douglas, and D. P. Mandic, "Adaptive frequency estimation in smart grid applications: Exploiting noncircularity and widely linear adaptive estimators," *IEEE Signal Processing Magazine*, vol. 29, no. 5, pp. 44–54, 2012.
- [17] J. Eriksson and V. Koivunen, "Complex random vectors and ICA models: Identifiability, uniqueness, and separability," *IEEE Trans. Information theory*, vol. 52, no. 3, pp. 1017–1029, 2006.
- [18] H. Li and T. Adali, "Complex-valued adaptive signal processing using nonlinear functions," *EURASIP Journal on Advances in Signal Processing*, vol. 2008, pp. 1–9, 2008.
- [19] B. Picinbono and P. Chevalier, "Widely linear estimation with complex data," *IEEE Trans. Signal Process.*, vol. 43, no. 8, pp. 2030–2033, 1995.
- [20] C. Jahanchahi, S. Kanna, and D. Mandic, "Complex dual channel estimation: Cost effective widely linear adaptive filtering," *Signal Processing*, vol. 104, pp. 33–42, 2014.
- [21] D. P. Mandic and V. S. L. Goh, *Complex valued nonlinear adaptive filters: noncircularity, widely linear and neural models*. John Wiley & Sons, 2009.
- [22] S. Chen, F. Cerda, P. Rizzo, J. Biela, J. H. Garrett, and J. Kovačević, "Semi-supervised multiresolution classification using adaptive graph filtering with application to indirect bridge structural health monitoring," *IEEE Trans. Signal Process.*, vol. 62, no. 11, pp. 2879–2893, 2014.
- [23] S. Chen, A. Sandryhaila, J. M. F. Moura, and J. Kovačević, "Signal denoising on graphs via graph filtering," in *Proc. of GlobalSIP*, 2014, pp. 872–876.
- [24] —, "Signal recovery on graphs: Variation minimization," *IEEE Trans. Signal Process.*, vol. 63, no. 17, pp. 4609–4624, Sept. 2015.
- [25] E. Isufi, A. Loukas, A. Simonetto, and G. Leus, "Autoregressive moving average graph filtering," *IEEE Trans. Signal Process.*, vol. 65, no. 2, pp. 274–288, 2017.
- [26] N. Perraudin and P. Vandergheynst, "Stationary signal processing on graphs," *IEEE Trans. Signal Process.*, vol. 65, pp. 3462–3477, 2017.
- [27] A. C. Yagan and M. T. Ozgen, "Spectral graph based vertex-frequency Wiener filtering for image and graph signal denoising," *IEEE Trans. Signal Inf. Process. Netw.*, vol. 6, pp. 226–240, 2020.
- [28] Z. Xiao and X. Wang, "Nonlinear polynomial graph filter for signal processing with irregular structures," *IEEE Trans. Signal Process.*, vol. 66, no. 23, pp. 6241–6251, 2018.
- [29] L. Ruiz, F. Gama, and A. Ribeiro, "Graph neural networks: Architectures, stability, and transferability," *Proceedings of the IEEE*, vol. 109, no. 5, pp. 660–682, 2021.
- [30] F. Gama, E. Isufi, G. Leus, and A. Ribeiro, "Graphs, convolutions, and neural networks: From graph filters to graph neural networks," *IEEE Signal Processing Magazine*, vol. 37, no. 6, pp. 128–138, 2020.
- [31] J. Mei and J. M. F. Moura, "Signal processing on graphs: Causal modeling of unstructured data," *IEEE Trans. Signal Process.*, vol. 65, no. 8, pp. 2077–2092, 2017.
- [32] F. Hua, R. Nassif, C. Richard, H. Wang, and A. H. Sayed, "Online distributed learning over graphs with multitask graph-filter models," *IEEE Trans. Signal Inf. Process. Netw.*, vol. 6, pp. 63–77, 2020.
- [33] A. Kroizer, Y. C. Eldar, and T. Routtenberg, "Modeling and recovery of graph signals and difference-based signals," in *Proc. of GlobalSIP*, Nov. 2019, pp. 1–5.
- [34] S. M. Kay, *Fundamentals of statistical signal processing: Estimation Theory*. Englewood Cliffs (N.J.): Prentice Hall PTR, 1993, vol. 1.
- [35] N. Geng, X. Yuan, and L. Ping, "Dual-diagonal LMMSE channel estimation for OFDM systems," *IEEE Trans. Signal Process.*, vol. 60, no. 9, pp. 4734–4746, 2012.
- [36] L. Dieci and T. Eiroa, "On smooth decompositions of matrices," *SIAM J. on Matrix Anal. and Appl.*, vol. 20, no. 3, pp. 800–819, 1999.
- [37] J. Serra and M. Najar, "Asymptotically optimal linear shrinkage of sample LMMSE and MVDR filters," *IEEE Trans. Signal Process.*, vol. 62, no. 14, pp. 3552–3564, 2014.
- [38] H. L. Van Trees, *Optimum array processing: Part IV of detection, estimation, and modulation theory*. John Wiley & Sons, 2004.
- [39] F. Rubio and X. Mestre, "Consistent reduced-rank LMMSE estimation with a limited number of samples per observation dimension," *IEEE Trans. Signal Process.*, vol. 57, no. 8, pp. 2889–2902, 2009.
- [40] C. Lameiro, I. Santamaría, P. J. Schreier, and W. Utschick, "Maximally improper signaling in underlay MIMO cognitive radio networks," *IEEE Trans. Signal Process.*, vol. 67, no. 24, pp. 6241–6255, 2019.
- [41] T. Adali, P. J. Schreier, and L. L. Scharf, "Complex-valued signal processing: The proper way to deal with impropriety," *IEEE Trans. Signal Process.*, vol. 59, no. 11, pp. 5101–5125, Nov. 2011.
- [42] C. Hellings and W. Utschick, "Combining linear estimation with scalar widely linear estimation," in *IEEE International Conference on Acoustics, Speech and Signal Processing (ICASSP)*, 2019, pp. 5177–5181.
- [43] T. Adali, H. Li, and S. Haykin, "Complex-valued adaptive signal processing," *Adaptive signal processing: next generation solutions*, 2010.
- [44] A. Monticelli, *State Estimation in Electric Power Systems: A Generalized Approach*. Boston, MA: Springer US, 1999, pp. 39–61, 91–101, 161–199.
- [45] G. B. Giannakis, V. Kekatos, N. Gatsis, S. J. Kim, H. Zhu, and B. F. Wollenberg, "Monitoring and optimization for power grids: A signal processing perspective," *IEEE Signal Processing Magazine*, vol. 30, no. 5, pp. 107–128, Sept. 2013.
- [46] S. Grotas, Y. Yakoby, I. Gera, and T. Routtenberg, "Power systems topology and state estimation by graph blind source separation," *IEEE Trans. Signal Process.*, vol. 67, no. 8, pp. 2036–2051, Apr. 2019.
- [47] D. Bienstock and A. Verma, "Strong NP-hardness of AC power flows feasibility," *Oper. Res. Lett.*, vol. 47, no. 6, pp. 494–501, 2019.
- [48] "Power systems test case archive." [Online]. Available: <http://www.ee.washington.edu/research/pstca/>